

**NAVAL POSTGRADUATE SCHOOL**  
**Monterey, California**



19980727 152

**THESIS**

**SPIN AND MAGNETISM: TWO TRANSFER  
MATRIX FORMULATIONS OF A CLASSICAL  
HEISENBERG RING IN A MAGNETIC FIELD**

by

Randall J. Franciose

June 1998

Thesis Advisor:  
Second Reader:

James H. Luscombe  
Robert L. Armstead

**Approved for public release; distribution is unlimited.**

# REPORT DOCUMENTATION PAGE

Form Approved  
OMB No. 0704-0188

Public reporting burden for this collection of information is estimated to average 1 hour per response, including the time for reviewing instruction, searching existing data sources, gathering and maintaining the data needed, and completing and reviewing the collection of information. Send comments regarding this burden estimate or any other aspect of this collection of information, including suggestions for reducing this burden, to Washington headquarters Services, Directorate for Information Operations and Reports, 1215 Jefferson Davis Highway, Suite 1204, Arlington, VA 22202-4302, and to the Office of Management and Budget, Paperwork Reduction Project (0704-0188) Washington DC 20503.

1. AGENCY USE ONLY (Leave blank)

2. REPORT DATE  
June 1998

3. REPORT TYPE AND DATES COVERED  
Master's Thesis

4. TITLE AND SUBTITLE  
**SPIN AND MAGNETISM: TWO TRANSFER MATRIX FORMULATIONS OF A CLASSICAL HEISENBERG RING IN A MAGNETIC FIELD**

5. FUNDING NUMBERS

6. AUTHOR(S)  
Franciose, Randall J.

7. PERFORMING ORGANIZATION NAME(S) AND ADDRESS(ES)  
Naval Postgraduate School  
Monterey, CA 93943-5000

8. PERFORMING ORGANIZATION  
REPORT NUMBER

9. SPONSORING / MONITORING AGENCY NAME(S) AND ADDRESS(ES)

10. SPONSORING / MONITORING  
AGENCY REPORT NUMBER

11. SUPPLEMENTARY NOTES

The views expressed in this thesis are those of the author and do not reflect the official policy or position of the Department of Defense or the U.S. Government.

12a. DISTRIBUTION / AVAILABILITY STATEMENT

Approved for public release; distribution is unlimited.

12b. DISTRIBUTION CODE

13. ABSTRACT (maximum 200 words)

Nanometer scale fabrication and experimental investigations into the magnetic properties of mesoscopic molecular clusters have specifically addressed the need for theoretical models to ascertain thermodynamic properties. Technological applications germane to these inquiries potentially include minimum scale ferromagnetic data storage and quantum computing. The one-dimensional nearest neighbor Heisenberg spin system accurately models the energy exchange of certain planar rings of magnetic ions. Seeking the partition function from which a host of thermodynamic quantities may be obtained, this thesis contrasts two transfer matrix formulations of a classical Heisenberg ring in a magnetic field. Following a discussion of the transfer matrix technique in an Ising model and a review of material magnetic characteristics, a Heisenberg Hamiltonian development establishes the salient integral eigenvalue equation. The 1975 technique of Blume *et al* turns the integral equation into a matrix eigenvalue equation using Gaussian numerical integration. This thesis alternatively proposes an exactly formulated matrix eigenvalue equation, deriving the matrix elements by expanding the eigenvectors in a basis of the spherical harmonics. Representing the energy coupling of the ring to a magnetic field with symmetric or asymmetric transfer operators develops pragmatically distinctive matrix elements; the asymmetric yielding a simpler expression. Complete evaluation will require follow-on numerical analysis.

14. SUBJECT TERMS

Nanomagnetism, Heisenberg Ring in a Magnetic Field, Magnetic Molecular Clusters, High-Spin Molecule Thermodynamics, Partition Function Generation Via Approximate Versus Exact Matrix Eigenvalue Equation Formulations

15. NUMBER OF PAGES

62

16. PRICE CODE

17. SECURITY CLASSIFICATION  
OF REPORT

Unclassified

18. SECURITY CLASSIFICATION  
OF THIS PAGE

Unclassified

19. SECURITY CLASSIFI-  
CATION OF ABSTRACT

Unclassified

20. LIMITATION OF  
ABSTRACT

UL



Approved for public release; distribution is unlimited

**SPIN AND MAGNETISM: TWO TRANSFER MATRIX FORMULATIONS OF A  
CLASSICAL HEISENBERG RING IN A MAGNETIC FIELD**

Randall J. Franciose  
Commander, United States Navy  
A.B., Assumption College, 1975

Submitted in partial fulfillment of the  
requirements for the degree of

**MASTER OF SCIENCE IN PHYSICS**

from the

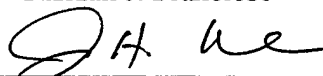
**NAVAL POSTGRADUATE SCHOOL  
June 1998**

Author:

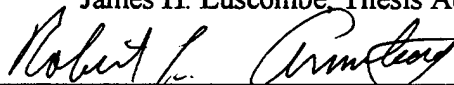


Randall J. Franciose

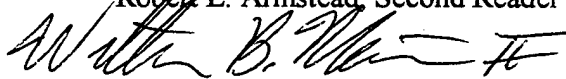
Approved by:



James H. Luscombe, Thesis Advisor



Robert L. Armstead, Second Reader



William B. Maier II, Chairman, Department of Physics



## ABSTRACT

Nanometer scale fabrication and experimental investigations into the magnetic properties of mesoscopic molecular clusters have specifically addressed the need for theoretical models to ascertain thermodynamic properties. Technological applications germane to these inquiries potentially include minimum scale ferromagnetic data storage and quantum computing. The one-dimensional nearest neighbor Heisenberg spin system accurately models the energy exchange of certain planar rings of magnetic ions. Seeking the partition function from which a host of thermodynamic quantities may be obtained, this thesis contrasts two transfer matrix formulations of a classical Heisenberg ring in a magnetic field. Following a discussion of the transfer matrix technique in an Ising model and a review of material magnetic characteristics, a Heisenberg Hamiltonian development establishes the salient integral eigenvalue equation. The 1975 technique of Blume *et al* turns the integral equation into a matrix eigenvalue equation using Gaussian numerical integration. This thesis alternatively proposes an exactly formulated matrix eigenvalue equation, deriving the matrix elements by expanding the eigenvectors in a basis of the spherical harmonics. Representing the energy coupling of the ring to a magnetic field with symmetric or asymmetric transfer operators develops pragmatically distinctive matrix elements; the asymmetric yielding a simpler expression. Complete evaluation will require follow-on numerical analysis.



## TABLE OF CONTENTS

I.	THE PURPOSE OF MAGNETIC MODELS .....	1
A.	INTRODUCTION	
	1. Historical Snapshot .....	1
	2. Models and Thermodynamics .....	1
B.	MESOSCOPIC MOLECULAR CLUSTERS .....	4
C.	TRANSFER MATRIX FOR AN ISING MODEL .....	8
D.	THESIS OBJECTIVES .....	10
II.	MAGNETIC PROPERTIES OF SOLIDS .....	13
A.	OVERVIEW .....	13
B.	ANGULAR MOMENTUM AND MAGNETISM .....	14
C.	SPIN ORBIT COUPLING, SHELL MODEL, AND HUND'S RULES .....	16
D.	MAGNETIZATION AND DIAMAGNETISM .....	19
E.	PARAMAGNETISM .....	20
	1. Langevin Function .....	21
	2. Pauli Paramagnetism .....	22
F.	FERROMAGNETISM.....	23
G.	ANTIFERROMAGNETISM AND FERRIMAGNETISM .....	25
H.	QUENCHED ORBITS AND THE HEISENBERG MODEL .....	26
III.	HEISENBERG SPIN SYSTEM FORMULATIONS .....	29
A.	OUTLINE .....	29
B.	TRANSFER MATRIX FOR CLASSICAL HEISENBERG SPINS .....	30
C.	ZERO-FIELD EIGENVALUES .....	34
D.	BLUME, HELLER, AND LURIE METHODOLOGY .....	36

E.	REPRESENTATION IN SPHERICAL HARMONICS .....	38
1.	The Symmetric Kernel .....	41
2.	The Non-Symmetric Kernel .....	43
IV.	DISCUSSION .....	47
	LIST OF REFERENCES .....	51
	INITIAL DISTRIBUTION LIST .....	53

# I. THE PURPOSE OF MAGNETIC MODELS

## A. INTRODUCTION

In matter, magnetic phenomena both originate from fundamental forces, and serve in ever increasing technological applications. Surprisingly however, there is no single comprehensive theory that can fully explain or accurately predict the full variety of material magnetic manifestations. For example, the entire theoretical edifice of Quantum and Statistical Mechanics cannot answer with certainty detailed questions of ferromagnetic coupling. It is known that ferro- and antiferromagnetism arise from short range interaction energy that forces spins of unpaired electrons into spontaneous alignment. [Ref. 1] More fundamentally, permanent magnetic moments are located in atoms or molecules and originate from the circling of the electrons around the nuclei (orbital moments) and from the spin of the electrons themselves (spin moments). These magnetic moments are proportional to angular momentum which is quantized as integral or half integral multiples of  $\hbar$ , (Planck's constant  $h \div 2\pi$ ). Particularly in the solid state, where electron orbits may be "quenched", the often intractable many body problem of "quantized gyroscope coupling", or energy exchanges in crystalline lattice structures has motivated a variety of models to explain experiment. [Ref. 2]

### 1. Historical Snapshot

In 1907 following Curie's work, Pierre Weiss [Ref. 3] proposed a theory of ferromagnetism in which magnetic moments interact with each other through an artificial molecular field proportional to the average magnetization. This type of theory is referred to as a "mean-field" theory; mean field theories have only limited accuracy but are often

useful as a first approach. Subsequent theories incorporated pairwise interaction of magnetic moments localized on fixed lattice sites with an energy that achieves a maximum value,  $J$ , when the moments are either aligned or anti-aligned. Two particular models characterizing this energy interaction are the Ising and the Heisenberg models. The Ising model assumes the magnetic moments are classical, one dimensional “sticks” capable of only two orientations. This mimics the behavior of  $S=\frac{1}{2}$  quantum spins. Later it was found that the Ising model could be applied to a wide range of systems that have an essential two-valued nature, such as binary alloys. The Heisenberg model regards the magnetic moments as being related to three-component quantum mechanical spin operators and assumes the interaction energy is proportional to the scalar product of these operators. There are other “spin” dimensional models but only a select few have been solved exactly for various space dimensionalities and external magnetic fields. Stanley [Ref. 4] provides an excellent comprehensive summary of these models, their applicability and limitations.

Neither the Ising nor the Heisenberg model has yielded as yet to an exact solution for a three dimensional (3-space) lattice. In 1944, in a landmark in the history of phase transitions and critical phenomena, Onsager [Ref. 5] solved the two-dimensional Ising model. An infinite-spin version of the 1-D Heisenberg model with free boundary conditions was solved by Fisher [Ref. 6] in 1964. Fisher showed that an infinite-spin Heisenberg model was equivalent to a classical version of the Heisenberg model in which the quantum spin operators are replaced by classical vectors of length  $\sqrt{S(S+1)}$  that are free to orient in any direction. This classical counterpart to the quantum Heisenberg model is called the classical Heisenberg model. The classical Heisenberg model should

apply to high-spin magnetic systems for all but extremely low temperatures. Fisher's student Joyce [Ref. 7] in 1967 published an exact solution to the zero-field one dimensional isotropic classical Heisenberg model with cyclic boundary conditions employing Wigner  $3j$  symbols. Blume et al [Ref. 8] in 1975 employed a transfer-matrix integral equation method and extended Joyce's work to tackle a 1-D classical Heisenberg system in an applied magnetic field. This thesis will follow and compare this latter method with a currently proposed method by Auslender [Ref. 9].

## 2. Models and Thermodynamics

These Ising and Heisenberg "toy models" enable reasonably accurate theoretical descriptions of certain physical systems and, significantly, shed valuable thermodynamic insight on some fluid and magnetic phase transformations. Statistical mechanics establishes a connection between the microscopic and macroscopic, or bulk, thermodynamic descriptions of a system. Central to statistical mechanical formulations is the partition function,

$$Z = \sum_{\text{all } \sigma} \exp(-\beta \mathcal{H}(\sigma)) \quad , \quad \text{where} \quad \beta = \frac{1}{k_B T} \quad , \quad (1.1)$$

$k_B$  is the Boltzmann constant,  $T$  is the absolute temperature, and  $\mathcal{H}$  is the energy Hamiltonian for each available quantum state,  $\sigma$ . As a summation of all Boltzmann factors, the partition function is the inverse proportionality factor between the probability of a particular energy state,  $P(\sigma)$  and each Boltzmann factor,

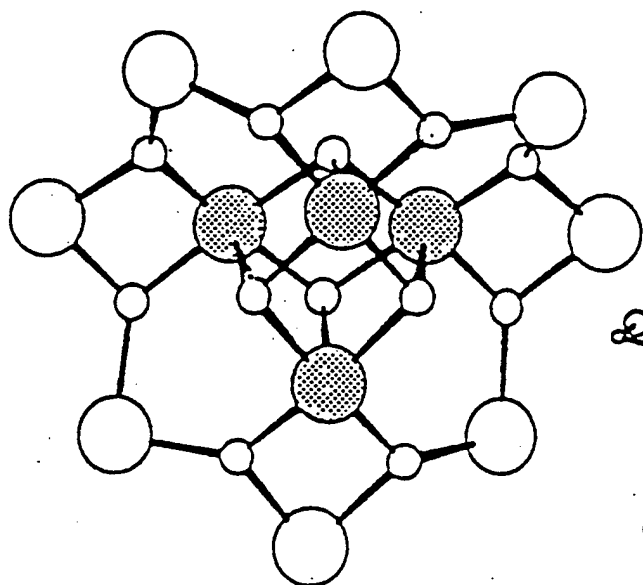
$$P(\sigma) = \frac{e^{-\beta \mathcal{H}(\sigma)}}{Z} \quad (1.2)$$

If ascertainable, the partition function is a very useful result. In fact, the partition function can be called the holy grail of equilibrium statistical mechanics because essentially an entire thermodynamic description of a system can be derived from this function. The generalized ensemble theory of Gibbs enables computing the complete set of thermodynamic quantities from purely mechanical properties of its microscopic constituents assuming only a “mechanical” structure, and obedience of Lagrange and Hamilton’s equations of motion [Ref. 10]. Thermodynamic averages such as entropy, average energy, heat capacity, magnetization and susceptibility, as well as the Gibbs potential and particularly the Helmholtz free energy are derived directly from the partition function. Of course, the essential completeness of the partition function necessitates a summation over all states; therefore, obtaining the partition function is no small challenge. This underscores the value of models that permit an exact determination of the partition function. A model can enable a theoretical calculation of state variables. Of course, a model’s validity and utility corresponds directly with its fidelity to reality.

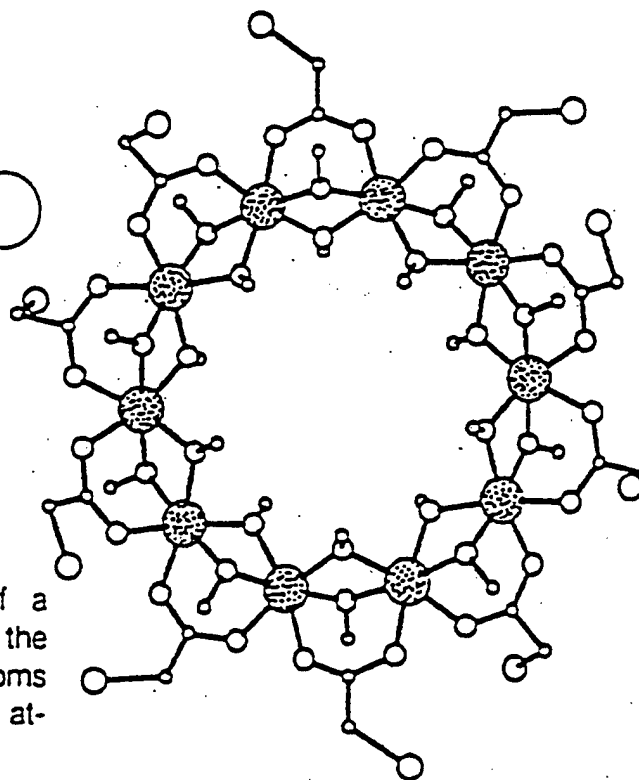
## **B. MESOSCOPIC MOLECULAR CLUSTERS**

Recently, fascinating experiments with large molecular clusters of metal ions provide an opportunity to employ a one dimensional Heisenberg spin model. Of interest is both the extremely clever and revealing experimental techniques and the particular scale (nanometer) of these investigations, where renormalization group theory [Ref. 11] had heretofore “coarse grained”, between atomic and bulk scales. These “mesoscopic” magnetic molecular clusters are enabling investigation of such behavior as quantum tunnelling of magnetization [Refs. 12, 13]. Some authors have forecast technological applications of these ultrasmall complexes in the field of both data storage and quantum

computing [Refs. 14, 15, 16] . Two molecular structures, depicted in Figure 1, are particularly noteworthy for their symmetry, high spin and revealing characteristics. The first contains twelve manganese ions, arranged in a ring of eight  $Mn^{3+}$  ions with spin  $S=2$  aligned parallel, enveloping the remaining four manganese  $Mn^{4+}$  atoms which form a tetrahedron with spins  $S=\frac{3}{2}$  in the opposite direction to the encircling octagon. This manganese acetate,  $Mn_{12}O_{12}(CH_3COO)_{16}(H_2O)_4$  is described as superparamagnetic,



Schematic view of the core of a  $[Mn_{12}O_{12}(\text{carboxylato})_{16}]$  cluster in which only the metal atoms and the bridging oxygen atoms (small circles) are shown. The manganese(IV) atoms are enhanced by the shadowing.



View of the ring structure of the  $Fe_{10}$  cluster, where the dotted circles represent the iron atoms and the empty circles are, in order of decreasing size, chlorine, oxygen, and carbon.

Figure 1. Two Mesoscopic molecular clusters, the manganese acetate on the left and the ferric wheel, right. (From Ref. 15)

having a ground state of  $S=10$  and the measured spin dynamics of this cluster in varying magnetic field reveals a hysteretic magnetic relaxation ascribed to resonant tunneling between quantum spin states. [Refs. 17, 18, 19] The second noteworthy molecular cluster is  $[\text{Fe}(\text{OCH}_3)_2(\text{O}_2\text{CCH}_2\text{CL})]_{10}$ , known as a “ferric wheel”. It contains 10 nearly coplanar  $\text{Fe}^{3+}$  ions each of spin  $S=5/2$ , symmetrically positioned on what constitutes a Heisenberg ring, a planar, one-dimensional spin system. In addition to this “ferric wheel” decagon, other iron molecular clusters have been synthesized, (e.g.  $\text{Fe}_8$ ,  $\text{Fe}_{17}$ ,  $\text{Fe}_{19}$ , as well as  $\text{Fe}_{10}$ ).

These molecular clusters would therefore seem to contain sufficiently few magnetic constituents that an exact determination of the partition function could be attempted. According to Gatteschi et al, however, [Ref. 15] when commenting on the quantum mechanical energy computations of these ferric rings:

A quantitative interpretation of the magnetic properties of these compounds has been possible only for  $\text{Fe}_8$ , and this at the cost of some effort [Ref. 20], the total number of states being 1,679,616. Exploiting symmetry allows the reduction of the problem to that of calculating 81 matrices, ranging in dimension from 1 to 4,170. A similar analysis proved to be impossible for the  $\text{Fe}_{17}$  or  $\text{Fe}_{19}$  clusters. Even with use of all the possible symmetries, the dimensions of the matrices remain much too large to be tackled with the standard approach. In this field, theoretical developments are strongly needed, so that we can interpret the thermodynamic properties of the new materials.

This clarion invitation to employ the theoretical Heisenberg spin model has been answered by Luscombe *et al*, [Ref. 21] astutely developing approximations for the relevant thermodynamic qualities. In [Ref. 21] it was shown that the classical Heisenberg model well approximated the observed thermodynamic properties of the “ferric wheel”

cluster with 10  $\text{Fe}^{3+}$  ions of spin  $S=5/2$ . This collaboration between theoretician and experimentalist was acknowledged by the latter in January, 1998, when Lasciafari *et al*, [Ref. 22] the leading research team in the field, effectively employed theoretical thermodynamic results from [Ref. 21] to advance the macromolecular magnetic frontier.

The continued development of these molecular magnetic systems, hopefully into useful nanomagnetic technologies, will clearly require reliable and robust theoretical techniques for predicting their thermodynamic properties. As noted above, it has been shown [Refs. 21 & 22] that approximate treatments based on classical Heisenberg spins can predict extremely well the observed magnetic behavior of small quantum Heisenberg systems. It is thus worthwhile to search for improved theoretical approaches to modeling the thermodynamic properties of classical Heisenberg spin systems. As will be discussed below, Blume's method [Ref. 8] for evaluating the partition function of the 1-D classical Heisenberg model in an applied magnetic field involves solving numerically an eigenvalue integral equation based on what is known as the transfer-matrix operator as its kernel. Using a numerical Gaussian integration technique, Blume *et al* transform the eigenvalue integral equation into a matrix eigenvalue equation. Auslender, [Ref. 9], has recently proposed an alternate strategy for solving the integral equation. Auslender's proposal is to represent the transfer-matrix operator in a basis set of spherical harmonics. As will be shown below, the spherical harmonics are the eigenvectors of the transfer-matrix operator for zero magnetic field in this basis set. Whether Auslender's proposal results in a more efficient method from a numerical point of view remains to be seen. In this thesis, we will, for the first time, set up the matrix representation of the transfer-

matrix operator in the spherical harmonic basis set. Since the transfer matrix method is key to the results of this thesis, we will review this method in the next section.

### C. TRANSFER MATRIX FOR AN ISING MODEL

Attributed to Kramers and Wannier [Ref. 23], the simplest illustration of the transfer-matrix technique is its application to the one dimensional nearest neighbor N-spin Ising model in a magnetic field. The physical justification will be presented in the next chapter, what follows simply demonstrates the math.

The 1-D nearest neighbor Ising Hamiltonian is defined by

$$\mathcal{H} = -J \sum_{i=1}^N \sigma_i \sigma_{i+1} - \frac{H}{2} \sum_{i=1}^N (\sigma_i + \sigma_{i+1}), \quad (1.3)$$

where  $\sigma_i = \pm 1$  is the randomly up or down oriented spin  $\frac{1}{2}$  Ising variable at lattice site  $i$ ,  $1 \leq i \leq N$ , and where  $J$  is the nearest neighbor exchange parameter, and  $H$  is the applied static magnetic field which is parallel or antiparallel to the moment of each “invertable” spin. Although an open Ising chain is solvable without recourse to the transfer-matrix method (e.g. Stanley [Ref. 4]), here we will instead assume periodic boundary conditions and define.  $\sigma_{N+1} = \sigma_1$ . Recalling equation (1.2), thermodynamic averages are constructed

from the probability distribution  $P(\sigma) = Z_N^{-1} \exp(-\beta \mathcal{H}(\sigma))$ , where  $\beta = (k_B T)^{-1}$ ,

and  $Z_N$  is the partition function,

$$Z_N(K, L) = \sum_{\{\sigma\}} \exp(-\beta \mathcal{H}(\sigma_i, \sigma_{i+1})) = \sum_{\{\sigma\}} \exp\left(K \sum_{i=1}^N \sigma_i \sigma_{i+1} + \frac{L}{2} \sum_{i=1}^N (\sigma_i + \sigma_{i+1})\right). \quad (1.4)$$

The notation  $\{\sigma\}$  indicates a summation over  $2^N$  spin configuration, i.e.

$\sum_{\{\sigma\}} \equiv \sum_{\sigma_1=-1}^1 \dots \sum_{\sigma_N=-1}^1$ , and  $K \equiv \beta J$  and  $L \equiv \beta H$  are dimensionless coupling constants.

Using the fact that Ising variables are classical "sticks" that will commute, the exponential of the sum is a product of the exponentials and (1.4) may be written,

$$Z_N(K, L) = \sum_{\{\sigma\}} T(\sigma_1, \sigma_2) T(\sigma_2, \sigma_3) \dots T(\sigma_{N-1}, \sigma_N) T(\sigma_N, \sigma_1), \quad (1.5)$$

where  $T(\sigma_i, \sigma_{i+1}) = \exp[K\sigma_i\sigma_{i+1} + \frac{L}{2}(\sigma_i + \sigma_{i+1})]$  which written out explicitly is a 2x2

*transfer matrix* with elements  $T(\sigma, \sigma')$ , each spin  $\sigma$  having possible values  $\pm 1$ ,

$$T \equiv \begin{pmatrix} T(+1, +1) & T(+1, -1) \\ T(-1, +1) & T(-1, -1) \end{pmatrix} = \begin{pmatrix} e^{K+L} & e^{-K} \\ e^{-K} & e^{K-L} \end{pmatrix}. \quad (1.6)$$

Then, summing over spins 2, ..., N in (1.5) the partition function is given by

$$Z_N = \sum_{\sigma_i = -1}^1 (T^N)_{\sigma_i \sigma_i} = \text{Trace } T^N, \quad (1.7)$$

that is the partition function of the N-spin Ising model with periodic boundary conditions is given as the trace of the N<sup>th</sup> power of the transfer matrix. Since the trace of a matrix is equal to the sum of its eigenvalues, and the eigenvalues of  $T^N$  are  $\lambda_1^N$  and  $\lambda_2^N$  where these are determined by the equation,

$$\begin{vmatrix} e^{K+L} - \lambda & e^{-K} \\ e^{-K} & e^{K-L} - \lambda \end{vmatrix} = 0 \text{ with solutions } \left. \begin{matrix} \lambda_1 \\ \lambda_2 \end{matrix} \right\} = e^K \cosh L \pm (e^{2K} \sinh^2 L + e^{-2K})^{\frac{1}{2}}, \quad (1.8)$$

we finally arrive at the result  $Z_N = \lambda_1^N + \lambda_2^N = \lambda_1^N \left( 1 - \left( \frac{\lambda_2}{\lambda_1} \right)^N \right)$ . (1.9)

Since  $\lambda_1 > \lambda_2$ , the second term in the parenthesis in (1.9) goes to zero for large N and can

be neglected. In zero magnetic field,  $H=0=L$ , (1.9) including both eigenvalues, yields

$$Z_N = 2^N (\text{Cosh}^N K + \text{Sinh}^N K). \quad (1.10)$$

This nearest neighbor Ising discrete spin system engenders a “2 by 2” transfer matrix. The nearest neighbor classical Heisenberg model however, has a continuously directable, all aspect spin system and the transfer “matrix” for continuous spins is an infinite matrix – or the kernel of an integral equation. Nevertheless, the eigenvalues of the transfer matrix allow one to obtain the partition function. We will discuss in Chapter III the application of the transfer-matrix method to the classical Heisenberg model.

#### D. THESIS OBJECTIVES

This thesis will contrast two methods of solving the one dimensional classical Heisenberg spin model. Blume and Auslender are the authors of the two techniques, the former acknowledged as the accepted method and the latter, a proposed alternative. Both Auslender’s and Blume’s methods are concerned with obtaining eigenvalues to the transfer matrix associated with the one-dimensional, nearest neighbor classical Heisenberg model in a magnetic field. Both methods seek the solutions of the eigenvalue equation:

$$\int ds' T(s, s') \psi_{l,m}(s') = \lambda_{l,m} \psi_{l,m}(s), \quad (1.11)$$

where  $T(s, s') = \exp\left(Ks \cdot s' + \frac{1}{2}L(s_z + s'_z)\right)$ ;  $ds = \sin \theta d\theta d\phi$ , and  $s, s'$  are adjacent three component spin vectors. Both methods seek the partition function for the N- spin system with periodic boundary conditions, which is given in terms of the eigenvalues

$$Z_N = \sum_{l,m} \lambda_{l,m}^N. \quad (1.12)$$

For zero magnetic field, the eigenvalues and eigenvectors are exactly obtainable as first shown by Joyce. [Ref. 7] In this case  $\lambda_{l,m} = 4\pi f_l(K)$  where  $f_l(K)$  are the modified spherical Bessel functions, and  $\psi_{l,m}(s) = Y_{l,m}(\theta, \phi)$ , the spherical harmonics.

Blume et al, (Heller and Lurie coauthors)[Ref.8], turn the integral eigenvalue equation into an  $M \times M$  matrix eigenvalue equation using  $M$ -point Gaussian integration. With a matrix size of  $16 \times 16$ , this technique results in a convergence to seven significant figures for the values of the Hamiltonian. Auslender also turns the integral equation into a matrix equation. The matrix in this case is obtained by expanding the eigenvectors using the spherical harmonics as a basis set. That is, he suggests expanding the eigenvectors in a magnetic field using zero-field eigenvectors. In principle, Auslender's matrix is infinite dimensional and must be truncated at some point. It is likely that a comparison of merit will only result from detailed numerical computations; however, this thesis will merely discuss formulations that reduce the integral equations to matrix eigenvalue equations employing both methods. Leading up to these formulations, any discussion of equilibrium statistical mechanics of the classical Heisenberg spin model must commence with formulating the energy exchange Hamiltonian. The transfer matrix will then lead to setting up the eigenvalue equation. There will be some discussion of zero magnetic field behavior and necessary discussion of integral equations, especially the role of a symmetric kernel. Representing the energy coupling of the Heisenberg ring to a magnetic field with symmetric or asymmetric transfer operators will be shown to result in mathematically equivalent but pragmatically distinctive element formulations.

Prior to this theoretical development in Chapter III, Chapter II will consist of a cursory review of the magnetic properties of matter following largely the excellent if old treatments of Von Hippel [Refs. 1&24], Kittel [Ref. 25], and Ashcroft & Mermin [Ref. 26].

## II. MAGNETIC PROPERTIES OF SOLIDS

### A. OVERVIEW

The magnetic properties of solids originate in the motion of the electrons and in the permanent magnetic moments of the atoms and electrons. This chapter will provide a review of magnetic characteristics and hopefully lead to a "motivation" of the Heisenberg model. Diamagnetism, which is very weak, arises from changes in the atomic orbital states induced by an applied magnetic field. Paramagnetism results from the presence of permanent atomic or electronic magnetic moments. Ferromagnetism, which is very strong, occurs when quantum mechanical exchange interactions align adjacent magnetic moments in the same direction. If the exchange interaction aligns the moments in opposite directions, and only one type of moment is present, cancellation occurs and the material is called anti-ferromagnetic. If two or more types of moments are present, there is a net moment equal to the difference and the material is called ferrimagnetic. Above some critical temperature, a phase transformation occurs and a ferro-, antiferro-, or ferrimagnetic material becomes paramagnetic. Ferro- and ferrimagnetic materials consist of domains or regions of completely magnetized material, separated by boundaries known as Bloch walls. According to Kittel [Ref. 25], and Hippel [Ref. 1], domain structure, dynamics, and boundary displacements are determined by various types of energies, such as magnetostatic energy, crystal anisotropy and magnetorestrictive energy. The complexity of these resultant forces contribute to the scientific and technological richness in this field. The succeeding paragraphs merely scratch the surface of these topics.

## B. ANGULAR MOMENTUM AND MAGNETISM

The relation between angular momentum and magnetism is based on the macroscopic observation that a current  $I$  circling an area  $A$  creates a magnetic field identical to that of a magnetic dipole. As such, the Bohr hydrogen atom's magnetic dipole,

$$|\mu| = IA = ev\pi r^2, \quad (2.1)$$

applies for an electron circling the proton  $v$  - times per second in an orbit of radius  $r$ .

For this same orbit the classical mechanical angular momentum,

$$|\mathbf{L}| = |m\mathbf{v} \times \mathbf{r}| = m2\pi r v r. \quad (2.2)$$

This angular momentum  $\mathbf{L}$  is antiparallel to  $\mu$  and combining (2.1) and (2.2) shows the

magnetic and angular moments are related as  $\mu = -\frac{e}{2m}\mathbf{L}$ .

Thus the magnetic and mechanical moments of circling electrons are interdependent and

the gyromagnetic ratio  $\gamma$  is classically defined  $\gamma \equiv \frac{|\mu|}{|\mathbf{L}|} = \frac{e}{2m}$ . (2.3)

At atomic scales, the Bohr magneton is considered an elementary magnetic moment with

$$|\mu_B| = \frac{e\hbar}{2m_e} = \gamma\hbar = 9.27 \times 10^{-24} \text{ in units amperes meter}^2 \text{ or joules/tesla} \quad (2.4)$$

(Note: of course, in measuring magnetic moments of nuclei, the nuclear magneton would

be a preferred unit and with a mass substitution,  $|\mu_N| = \frac{1}{1836}|\mu_B|$ )

If the magnetic moment is measured in Bohr magnetons and angular momentum in units of  $\hbar$ , the ratio of magnetic to mechanical moment, known as the dimensionless  $g$ -factor,

(for the classically single orbiting electron),  $g = \frac{\mu}{\mathbf{L}} \frac{\hbar}{\mu_B} = \gamma \frac{\hbar}{\mu_B} = 1$

In a magnetic field  $\mathbf{B}$ , the permanent magnetic moments will experience a torque

$$\vec{\tau} = \vec{\mu} \times \mathbf{B} = \frac{d\mathbf{L}}{dt}, \quad \text{but } \mathbf{L} = \frac{-2m}{e} \vec{\mu}, \quad \text{and thus } \frac{d\vec{\mu}}{dt} = \frac{-e}{2m} \vec{\mu} \times \mathbf{B} = -\gamma \vec{\mu} \times \mathbf{B} \quad (2.5)$$

For a static field applied in the  $+\hat{z}$  direction, taking the cross product followed by the second time derivatives, yields the component equations of (2.5):

$$\ddot{\mu}_x = -(\gamma B)^2 \mu_x, \quad \ddot{\mu}_y = -(\gamma B)^2 \mu_y, \quad \dot{\mu}_z = 0. \quad (2.6)$$

Solutions of (2.6) are:  $\mu_x = A \cos \omega_z t$ ,  $\mu_y = A \sin \omega_z t$ , and  $\mu_z = \text{const}$ , where

$\omega_z = \gamma B$  and  $\omega_z / 2\pi = \nu_m$  is called the Larmor frequency. Hence these two oscillating

components are  $90^\circ$  out of phase and add to a circular rotation in the  $x$ - $y$  plane. The

magnetic moment precesses around the magnetic field axis with a frequency proportional

to the field strength but independent of position.

The Larmor frequency is not quantized but three quantum numbers are integer multiples of  $\hbar$ . The boundary conditions on the time independent Schrödinger wave equation restrict the quantum numbers as follows. The principle quantum number  $n$  is allowed positive integer values 1,2,3,... The orbital angular momentum quantum number

$\ell$  can take integer values  $0 \leq \ell < n$ . Quantum mechanically the total orbital angular

momentum  $\equiv \mathbf{L} = \sqrt{\ell(\ell+1)}\hbar$ . The magnetic field directed component of  $\mathbf{L} = L_z = m\hbar$ ,

where the magnetic quantum number,

$$m = \sqrt{\ell(\ell+1)} \cos \theta, \quad (2.7)$$

with  $m = \ell, \ell-1, \dots, -(\ell-1), -\ell$ , and  $\theta$  the quantized polar angle between the  $\mathbf{B}$  field

and  $L$ .

The quantized magnetic moment in the magnetic field has a potential energy

$$U = -\boldsymbol{\mu} \cdot \mathbf{B} = \mu B \cos \theta = -\sqrt{\ell(\ell+1)} \mu_B \|B\| \cos \theta = m \mu_B B. \quad (2.8)$$

The electron itself, has intrinsic angular momentum and thus creates a magnetic moment  $\bar{\mu} = -g_e \frac{e}{2m} \mathbf{S}$  where the electronic “ $g_e$ ” factor was predicted by Dirac to equal approximately 2, has been measured experimentally to 2.0023, and is given [Ref.26] by,

$$g_e = 2 \left[ 1 + \frac{\alpha}{2\pi} + O(\alpha^2) + \dots \right], \alpha, \text{ the fine structure constant} = \frac{e^2}{4\pi\epsilon_0 \hbar c} \approx \frac{1}{137}. \quad (2.9)$$

Using the electronic spin “ $g$ ” factor equal to twice the orbital, then classically the

$$\text{permanent magnetic dipole moment } \boldsymbol{\mu} = -\gamma(\mathbf{L} + 2\mathbf{S}). \quad (2.10)$$

### C. SPIN ORBIT COUPLING, SHELL MODEL, AND HUND'S RULES

The combined angular momentum produced by the spin and orbital motion is  $\mathbf{J} = \mathbf{L} + \mathbf{S}$ . The total angular momentum  $\mathbf{J}$  is always a good quantum number, (i.e. commutes with the Hamiltonian), but  $\mathbf{L}$  and  $\mathbf{S}$  are good only to the extent that spin – orbit coupling is unimportant [Ref. 26]. Both the spin and orbital angular moments will tend to precess around  $\mathbf{J}$  and,

$$J^2 = (\mathbf{L} + \mathbf{S})^2 = L^2 + S^2 + 2\mathbf{L} \cdot \mathbf{S} = \ell(\ell+1)\hbar^2 + \frac{3}{4}\hbar^2 + 2\mathbf{L} \cdot \mathbf{S} \quad (2.11)$$

The vector addition first solved by Landé results in the  $g$  – factor for  $L$ - $S$  coupling

$$g = (\mathbf{L} + 2\mathbf{S}) \cdot \mathbf{J} / J^2 = 1 + \frac{J(J+1) + S(S+1) - L(L+1)}{2J(J+1)} \quad (2.12)$$

where this Landé  $g$ - factor is relevant in the expression  $\boldsymbol{\mu} = -g\mu_B \mathbf{J} / \hbar$ .

Glibly allowing that the colossal variety of not only magnetic effects, but of all nature's splendor derives quantum mechanically from the atomic shell model, angular momenta coupling and shell filling configurations are key to understanding this process. Deriving from the Pauli exclusion principle or the antisymmetry of fermion wave functions, the underlying quantum mechanical justification of shell filling, selection rules, ionization potentials, electron affinities and atomic bonds are beyond the scope of this thesis, but brief essentials relevant to magnetic properties follow. Filled shells will have zero orbital, spin, and total angular momentum, and consequently zero permanent magnetic moment. For ground states in partially filled shells, the order of filling obey the Pauli exclusion principle and is roughly governed by Hund's rules which are as follows:

Rule 1. In placing  $n$  electrons into the  $2(2\ell + 1)$  levels of the partially filled shell, those that lie lowest in energy have the largest total spin  $S$ ; thus if possible, the first  $2\ell+1$  of allowed electrons in a shell will align spin-up.

Rule 2. The total orbital angular momentum  $L$  of the lowest lying states has the largest value that is consistent with Rule 1 and the exclusion principle

Rule 3. Total angular momentum  $J = \sqrt{J(J+1)}$  where  $J$  takes on integral values between  $|L - S|$  if the shell is less than half full and  $L + S$  if more than half full.

Russel-Saunders coupling applicable to lighter elements and favored in the d-shell and f-shell, is represented by a term in the Hamiltonian of the form  $\lambda(\mathbf{L} \cdot \mathbf{S})$ . This spin-orbit coupling will favor maximum  $J$  (parallel orbital and spin angular momenta) if  $\lambda$  is negative, and minimum  $J$  (antiparallel orbital and spin momenta) if  $\lambda$  is positive. As it turns out,  $\lambda$  is positive for shell that are less than half filled and negative for shells more

than half filled. The configurations of ground state d-shell and f-shell ions are tabulated below. The "multiplets" notation  $^{2S+1}X_J$ , where ( $X=L$  in the 'SPDF' spectroscopic code), conveys  $S$ ,  $L$ , and  $J$ , and the shell filling order for solids of magnetic interest illustrate Hund's rules.

d-shell ( $l = 2$ )								
$n$	$l_z = 2,$	$1,$	$0,$	$-1,$	$-2$			
1	↓					$1/2$		
2	↓	↓				$1$		
3	↓	↓	↓			$3/2$		
4	↓	↓	↓	↓		$2$		
5	↓	↓	↓	↓	↓	$5/2$		
6	↑↓	↑	↑	↑	↑	$2$		
7	↑↓	↑↓	↑	↑	↑	$3/2$		
8	↑↓	↑↓	↑↓	↑	↑	$1$		
9	↑↓	↑↓	↑↓	↑↓	↑	$1/2$		
10	↑↓	↑↓	↑↓	↑↓	↑↓	$0$		
						$L =  \Sigma l_z $		
						$J$		
						SYMBOL		
						$3/2$	} $J =  L - S $	${}^2D_{3/2}$
						$2$		${}^3F_2$
						$3/2$		${}^4F_{3/2}$
						$0$		${}^5D_0$
						$5/2$		${}^6S_{5/2}$
						$4$	} $J = L + S$	${}^5D_4$
						$9/2$		${}^4F_{9/2}$
						$4$		${}^3F_4$
						$5/2$		${}^2D_{5/2}$
						$0$		${}^1S_0$
f-shell ( $l = 3$ )								
$n$	$l_z = 3,$	$2,$	$1,$	$0,-1,-2,-3$				
1	↓					$1/2$		
2	↓	↓				$1$		
3	↓	↓	↓			$3/2$		
4	↓	↓	↓	↓		$2$		
5	↓	↓	↓	↓	↓	$5/2$		
6	↓	↓	↓	↓	↓	$3$		
7	↓	↓	↓	↓	↓	$7/2$		
8	↑↓	↑	↑	↑	↑	$3$		
9	↑↓	↑↓	↑	↑	↑	$5/2$		
10	↑↓	↑↓	↑↓	↑	↑	$2$		
11	↑↓	↑↓	↑↓	↑↓	↑	$3/2$		
12	↑↓	↑↓	↑↓	↑↓	↑	$1$		
13	↑↓	↑↓	↑↓	↑↓	↑	$1/2$		
14	↑↓	↑↓	↑↓	↑↓	↑↓	$0$		
						$L =  \Sigma l_z $		
						$J$		
						SYMBOL		
						$5/2$	} $J =  L - S $	${}^2F_{5/2}$
						$4$		${}^3H_4$
						$9/2$		${}^4I_{9/2}$
						$4$		${}^5I_4$
						$5/2$		${}^6H_{5/2}$
						$0$	} $J = L + S$	${}^7F_0$
						$7/2$		${}^8S_{7/2}$
						$6$		${}^7F_6$
						$15/2$		${}^6H_{15/2}$
						$8$		${}^5I_8$
						$15/2$	${}^4I_{15/2}$	
						$6$	${}^3H_6$	
						$7/2$	${}^2F_{7/2}$	
						$0$	${}^1S_0$	

<sup>a</sup>↑ = spin 1/2; ↓ = spin -1/2.

Table 1. Ground states of ions with partial d- or f-shells per Hund's rules<sup>a</sup> [From Ref.26]

#### D. MAGNETIZATION AND DIAMAGNETISM

The magnetic induction  $\mathbf{B}$  in free space is related to the field strength or magnetic intensity by  $\mathbf{B} = \mu_0 \mathbf{H}$  where  $\mu_0 = 4\pi \times 10^{-7}$  henry/meter is called the permeability of vacuum. In a solid material  $\mathbf{B} = \mu \mathbf{H}$ , which alternatively can be expressed as,

$$\mathbf{B} \equiv \mu_0 (\mathbf{H} + \mathbf{M}) = \mu \mathbf{H}. \quad (2.13)$$

(Note: Of course,  $\mu$  here is the permeability of the solid not a dipole moment.)  $\mathbf{M}$  is called the magnetization of the solid, the term  $\mu_0 \mathbf{M}$  equals the extra magnetic induction due to the material.  $\mathbf{M}$  in fact, is equivalent to the density of magnetic dipole moment or dipole moment per unit volume. The magnetization is also proportional to the applied field and the factor of proportionality is called the susceptibility. The magnetic susceptibility per unit volume is defined as  $\chi = \mathbf{M}/\mathbf{H}$ . (2.14)

Substances with a negative magnetic susceptibility demonstrate diamagnetism which is a material manifestation of Lenz's Law, which in effect orients Faraday induction such that "a current induced by a changing field will always oppose the change that induces it." With zero angular momentum, fully closed shells have zero permanent moments, (eq 2.10), but in an external magnetic field, there is an induced moment. The averaged induced magnetic moment for each electron equals,

$$\mu_{\text{induced}} = \frac{e^2 \langle r \rangle^2}{6m} \mathbf{B}, \quad (2.15)$$

where  $e$  and  $m$  equal the electron charge and mass and  $\langle r \rangle$  is the average electron orbital radius. Diamagnetism in most solids is very weak with susceptibilities on the order of  $10^{-5}$ . It is generally only observed when other types of magnetism are totally absent. The variety of net magnetic susceptibilities in matter is illustrated by Figure 2.

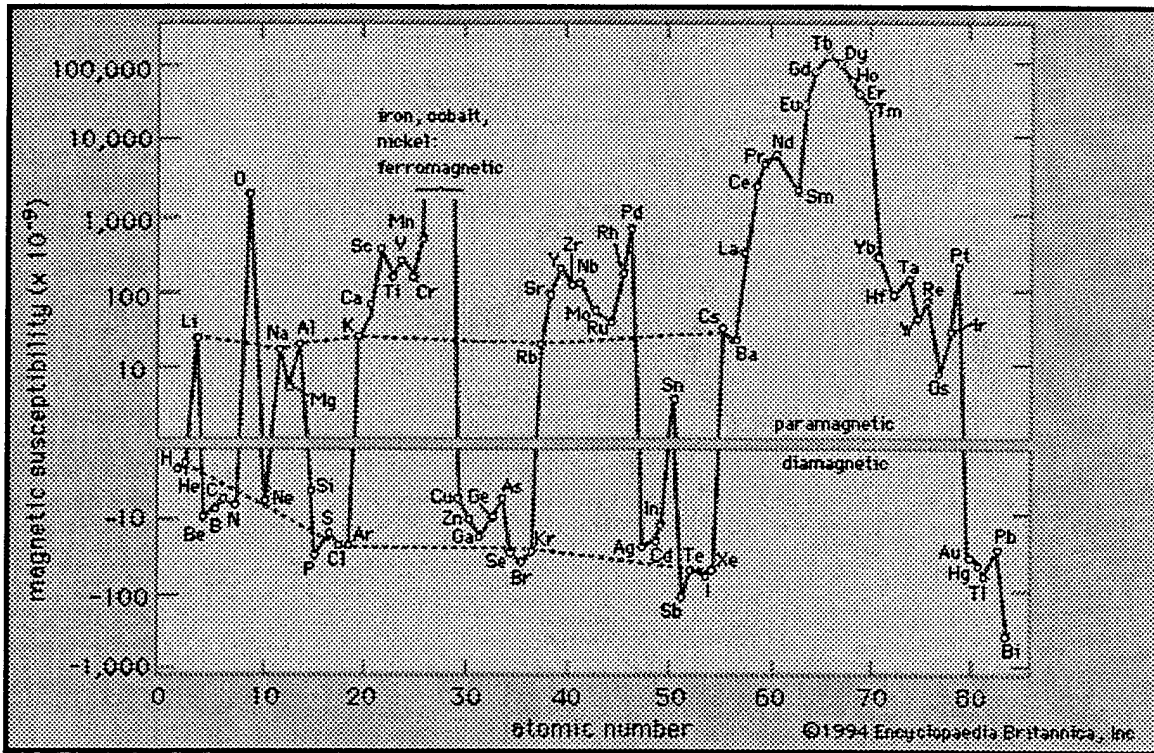


Figure 2. Diamagnetic elements in lower portion, paramagnetic in upper [From Ref. 27]

## E. PARAMAGNETISM

Positive susceptibilities ( $\chi > 0$ ) are generally termed paramagnetic. Permanent magnetic moments give rise to paramagnetism, and per Kittel [Ref. 25], electronic paramagnetism is found in :

- All atoms and molecules possessing an odd number of electrons, since the total spin of the system cannot go to zero.
- All free atoms and ions with a partly filled inner shell: transition elements, rare earth and actinide elements.
- A few miscellaneous compounds with an even number of electrons, including molecular oxygen and organic biradicals.
- Most but not all metals as depicted in Figure 2.

What follows is a Maxwell Boltzmann distribution treatment of the Langevin Theory of paramagnetism.

### 1. Langevin Function

Permanent magnetic moments tend to orient in magnetic fields. With  $N$  atoms per unit volume, each bearing a magnetic moment  $\mu$ , magnetization results from the orientation of these moments in an applied field. Thermal disorder resists this orientation tendency. The energy of interaction with an applied magnetic field  $H$  is

$E = -\mu \cdot \mathbf{H} = -\mu H \cos\theta$ , where  $\theta$  is between the moment and the field direction. The

magnetization will be  $\mathbf{M} = N\mu \overline{\cos\theta}$  where  $N$  is the density and  $\overline{\cos\theta}$  is the average over a distribution in thermal equilibrium. According to Boltzmann distribution, the relative probability of finding a molecule in a solid angle element  $d\Omega$  is proportional to

$e^{-E/kT}$ , and  $\overline{\cos\theta} = \int e^{-E/kT} \cos\theta d\Omega \div \int e^{-E/kT} d\Omega$ . Over all solid angles,

$$\overline{\cos\theta} = \frac{\int_0^\pi 2\pi \sin\theta \cos\theta e^{\mu H \cos\theta/kT} d\theta}{\int_0^\pi 2\pi \sin\theta e^{\mu H \cos\theta/kT} d\theta} \quad (2.16)$$

letting  $x = \cos\theta$  and  $a = \mu H/kT$ , then

$$\overline{\cos\theta} = \frac{\int_{-1}^1 e^{ax} x dx}{\int_{-1}^1 e^{ax} dx} = \frac{d}{da} \ln \int_{-1}^1 e^{ax} dx = \coth a - \frac{1}{a} \equiv L(a). \quad (2.17)$$

$L(a)$  is called the Langevin function. When the field energy is small in comparison with  $kT$ ,  $a \ll 1$ , then  $L(a) \sim a/3$  and  $\mathbf{M} \approx N\mu^2 \mathbf{H}/3kT$  (2.18)

The magnetic susceptibility in the limit as  $\mu H/kT \ll 1$  is

$$\chi = M/H = N\mu^2/3kT = C/T, \quad (2.19)$$

where the Curie constant  $C = N\mu^2/3k$ . The inverse temperature dependence is known

as the Curie law and the entire expression is called the Langevin equation. This Langevin derivation is entirely classical with unrestricted space orientation of the moments in a magnetic field and furthermore, depends intrinsically on the Maxwell Boltzmann distribution. A quantum theory of paramagnetism still employing the Boltzmann distribution uses the Landé g factor (2.12) and what is known as the Brillouin function for calculating the  $2J+1$  discrete and equally placed energy levels in the field.

Essentially equivalent to the Curie Law, the calculation yields  $\chi = Np^2 \mu_B^2 / 3kT$ , where the effective number of Bohr magnetons is defined as  $p = g[J(J+1)]^{1/2}$ .

## 2. Pauli Paramagnetism

The Langevin equation does not apply to conduction electrons which obey the Fermi-Dirac distribution. Conduction electrons are neither spatially localized like electrons in partially filled ionic shells, nor because of stringent constraints of the exclusion principle, do they respond independently like electrons localized on different ions [Ref. 26]. Although small, Pauli paramagnetic susceptibility results from the coupling of intrinsic electron spins with an applied field  $\mathbf{H}$ . There is also a diamagnetic effect arising from the coupling of the field to the orbital electron motion. This is called Landau diamagnetism and for *free* electrons in metals, the susceptibility,

$\chi_{Landau} = -\frac{1}{3} \chi_{Pauli}$  The resulting net susceptibility for  $N$  conduction electron is

$\chi = N\mu_B^2 / E_F$ , where  $E_F$  is the Fermi level. Pauli paramagnetism is independent of temperature and even at room temperature is hundreds of times smaller than the paramagnetism of magnetic ions. Paramagnetism usually masks the atomic diamagnetism present in solids. In practice, it is the total susceptibility that is revealed by

a measurement of bulk moment induced by a field and this is a combination of the Pauli paramagnetic susceptibility, the Landau diamagnetic susceptibility, and the Larmor diamagnetic susceptibility (of the closed-shell ion cores). As a result, isolating experimentally these particular terms of the susceptibility is not at all straightforward. Nuclear magnetic resonance (NMR) is one such technique that enables experimental discrimination of these susceptibilities. Like NMR which can measure spin-lattice relaxation rates, another technique called muon spin relaxation, also is central to the current investigations of magnetic molecular clusters cited in the introduction [Ref. 22]. Unlike these recent frontier if somewhat esoteric inquiries, the next section will attempt to describe a more prosaic phenomena, namely refrigerator magnets.

## F. FERROMAGNETISM

The transition metals Fe, Co and Ni, rare earth metals such as Gd and a few oxides such as  $\text{CrO}_2$  and  $\text{ErO}$  display very large magnetization. These ferromagnetic materials contain permanent atomic magnetic dipoles, the difference from a paramagnetic substance being that, below a certain temperature, the dipoles retain parallel orientation even in the absence of an external field. Figure 3a. depicts a magnetization curve of a ferromagnetic material. This hysteresis loop characterizes the magnetic induction  $B$  as a "*function*" of the applied field  $H$ . As the applied field  $H$  is increased,  $B$  begins to increase slowly. The slope rises sharply as  $B$  rapidly increases until the saturation induction. Upon decreasing the field, the original curve is not retraced. At  $H$  equal to zero, the specimen is still magnetized with the remanent induction. Here is the reason that zero field permanent magnets are able to emblazon refrigerators. If  $H$  is now made

negative, when  $B=0$  indicates the coercive force required to de-magnetize the material. The symmetric curve depicts saturation, remanence and coercive force for negative induction values. This irreversible double valued hysteresis is the signature behavior of ferromagnetic materials. The work required to go around the hysteresis loop once is proportional to the enclosed area. Technologically an alloy with a fat loop (Figure 3b.) makes a good permanent magnet; whereas a thin loop, (Figure 3c.) with small area, demagnetizes rapidly and makes an efficient AC transformer element.

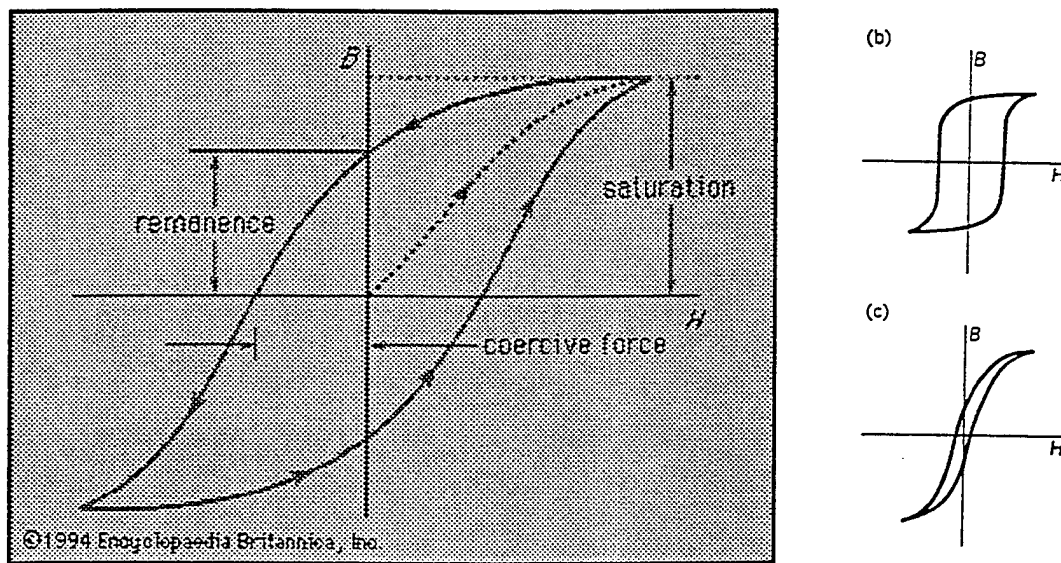


Figure 3. Hysteresis curves for (a) soft iron, (b) a good permanent magnet, and (c) an alloy suitable for use in a power transformer. [From Ref. 27]

The source of ferromagnetism is a parallel alignment of unpaired electron spins. As noted in the introduction, Weiss (1907) postulated a molecular field to explain ferromagnetism and he further postulated domain formation to explain the hysteretic magnetization curve. The molecular Weiss field was formulated as  $\mathbf{H}_w = \lambda \mathbf{M}$ , where  $\lambda$  is termed the Weiss constant and this field is added to the applied field  $\mathbf{H}$  in Curie's Law (eq 2.18).

Then the magnetization,

$$\mathbf{M} = \frac{C}{T}(\mathbf{H} + \lambda\mathbf{M}), \text{ and solving for } \frac{|\mathbf{M}|}{|\mathbf{H}|} = \frac{M}{H} = \chi = \frac{C}{T - \lambda C} = \frac{C}{T - T_c}, \quad (2.20)$$

where  $T_c$  the Curie temperature, is where the transformation from the paramagnetic to the ferromagnetic occurs. The domain hypothesis can be inferred from the hysteresis curve and were observed in fact some twenty five years later in 1931. Within domains, all moments are aligned but there is random orientation of the domains resulting in a net magnetization of zero. The external magnetic field induces magnetization via domain wall motion. The applied external field will cause favorably aligned domains to grow thereby shrinking unfavorably oriented domains. Rotation of other domain moments maximizes the magnetization. The saturation value corresponds essentially to single domain status. When the field is removed, the specimen remains magnetized. Although domains typically tend to rotate back, the large aligned domains do not easily revert to the original random arrangement. Reduction and reversal of the field allow a domain pattern to return, depending on the ease with which domain walls can nucleate, move through the material, and again be ejected.

## G. ANTIFERROMAGNETISM AND FERRIMAGNETISM

There are two other important classes of magnetic behavior. When adjacent unpaired spins are aligned in an opposite fashion, the resultant phenomenon is called antiferromagnetism. The susceptibility is then positive and increases as the temperature increases since thermal energy as always disrupts long range order. Figure 4. compares alignment of magnetic moments and temperature effects on ferro- and antiferromagnetic materials. The peak in the susceptibility  $\chi$  versus temperature  $T$  in Figure 4b. is called

the Neel temperature  $\Theta_N$  and corresponds to the Curie temperature in ferromagnetic materials. A class of complex oxides known as spinels, having the composition  $XOFe_2O_3$  (where X is a metal), exhibit ferromagnetic interaction yet have anti-parallel spins as depicted in Figure 4c. A net moment results since the opposite spins are unequal. The magnetization of these spinels, known as ferrites, have wide application in the electronics industry.

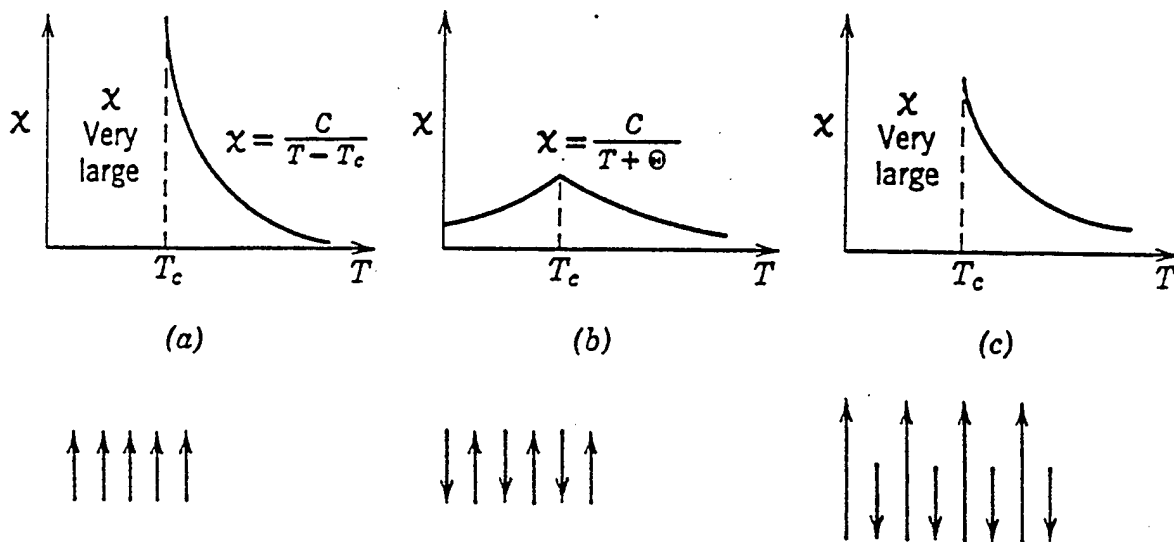


Figure 4. Magnetic susceptibility versus  $T$  for (a) ferromagnetic, (b) antiferromagnetic, and (c) ferrimagnetic materials, with magnetic moment alignments indicated for each case. [After Ref. 1]

## H. QUENCHED ORBITS AND THE HEISENBERG MODEL

The moments of ferromagnetic arrays could in principle stem from orbital moments as well as spin moments of individual electrons. However, since crystal structures are held together by electron bonds, it is not surprising to discover from magnetomechanical measurements that the orbital moments are essentially quenched by such bond formation. The gyromagnetic ratio for orbital moments is  $e/2m$  (eq. 2.3); for

ferromagnetics, it proves to be about  $e/m$ , the value of electron spins. Although the contribution of orbital moments to the saturation magnetization is generally only 5-10% of the total, they are nonetheless important as a source of magnetic crystal anisotropy [Ref. 1]. A quantum mechanical explanation for the Weiss field proposed by Heisenberg (1928), involves an exchange interaction between neighboring electron spins. The exchange energy explanation may be motivated by the Pauli exclusion principle and corresponding Fermi Dirac statistics requiring distinction of each electronic state by its own unique set of quantum numbers. Overlapping wave functions can lead to a decrease in over-all energy in certain cases, and therefore favor a parallel alignment of spins. The spin quantum number corresponds to up or down, hence inversion from parallel to antiparallel leads to a new electron cloud of different electrostatic energy. Bohm [Ref.28] concurs and attributes the antisymmetry of the complete electronic wave function with prescribing parallel or antiparallel spin alignments. Furthermore the energy, apparently a result of spin interactions, is actually a result of the correlation between mean coulomb energy and spin.

Ashcroft and Mermin [Ref. 26] construct a spin Hamiltonian for a two electron system noting that each individual electron spin operator satisfies  $S_i = \frac{1}{2} \left( \frac{1}{2} + 1 \right) = \frac{3}{4}$ ,

so that total S satisfies ,

$$S^2 = (S_1 + S_2)^2 = \frac{3}{2} + 2S_1 \cdot S_2, \quad (2.21)$$

since  $S^2$  has eigenvalues  $S(S+1)$  in states of spin S, the operator  $S_1 \cdot S_2$  has eigenvalue  $-\frac{3}{4}$

in the singlet ( $S=0$ ) state and  $+\frac{1}{4}$  in the triplet ( $S=1$ ) states. Consequently the operator

$\mathcal{H}^{\text{spin}} = \frac{1}{4}(E_s + 3E_t) - (E_s - E_t)\mathbf{S}_1 \cdot \mathbf{S}_2$  has eigenvalue  $E_s$  in the singlet and  $E_t$  in each of

the triplet states and is the desired Hamiltonian. By redefining the zero of energy, the constant, common to all four states,  $(E_s + 3E_t)/4$  can be omitted and the spin

Hamiltonian is  $\mathcal{H}^{\text{spin}} = -J\mathbf{S}_1 \cdot \mathbf{S}_2$ ,  $J = E_s - E_t$ . (2.22)

Seeking lowest energy, the scalar product of the vector spin operators will favor parallel spins if  $J$  is positive and antiparallel if  $J$  is negative. It is also noteworthy that in contrast to dipolar interaction, the coupling in this spin Hamiltonian depends only on the relative orientation of the two spins and not on the vector difference between the spins. It is remarkably true that in many cases of interest, the form of the spin Hamiltonian is simply that for the two spin case summed over all pairs of ions,

$$\mathcal{H}^{\text{spin}} = -\sum J_{ij} \mathbf{S}_i \cdot \mathbf{S}_j \quad (2.23)$$

This expression (2.23) is called the Heisenberg Hamiltonian and the  $J_{ij}$  are the exchange coupling constants. Stanley [Ref. 4] points out that this model is not valid for a wide variety of real magnetic materials as it assumes:

- a) Well localized spins (i.e. small wave function overlap)
- b) Complete isotropy of interaction.

The 3d transition metals have overlapping wave function and rare earth metals are generally anisotropic. Nonetheless, the Heisenberg spin Hamiltonian formulation can yield fruitful theoretical information in many cases, one such being the mesoscopic "Ferric" Wheels.

### III. HEISENBERG SPIN SYSTEM FORMULATIONS

#### A. OUTLINE

This chapter will contrast two theoretical approaches to obtaining the partition function for a one-dimensional nearest neighbor classical Heisenberg spin system in a magnetic field. At the outset, section B will develop the symmetric and non-symmetric transfer operators, and show that the partition function for an  $N$ -spin system is equal to the sum of the " $N^{\text{th}}$ -power raised" transfer matrix eigenvalues. Next section C will delineate the zero field analytic solution of a classical Heisenberg ring. Then, tackling a finite magnetic field in Section D, the numerical integration approach of Blume *et al* will be described, following directly the authors' formulation. Section E will suggest a new approach to solving the classical Heisenberg spin system. The matrix eigenvalue equation will be constructed by representing the transfer operator kernel in a basis of spherical harmonics, (which are the zero field eigenvectors in the analytic solution). The infinite matrix that results will be examined qualitatively for both zero and non-zero field characteristics. Development using first a symmetric magnetic field transfer operator, followed by and compared with a non-symmetric transfer operator expansion, employ both integral equation and rotation group mathematics. The non-symmetric transfer operator surprisingly yields a simpler matrix construction and both formulations enable a conceptual contrasting to Blume *et al* while setting the stage for an actual calculational comparison.

## B. TRANSFER MATRIX FOR CLASSICAL HEISENBERG SPINS.

The starting point in this development is the Heisenberg Hamiltonian, which is a summation of quantum spin operators in units of  $\hbar$ :

$$\mathcal{H} = -J \sum_{i=1}^N \mathbf{S}_i \cdot \mathbf{S}_{i+1}, \text{ where } \mathbf{S}_{N+1} \equiv \mathbf{S}_1 \text{ (periodic boundary conditions), and } J \text{ is the}$$

unique exchange interaction energy applicable to each adjacent pair. It is noteworthy to recall equation (2.22), that in this formulation ( $J < 0$ )  $J > 0$  promotes (anti-) ferromagnetic ordering at low temperatures. To incorporate system coupling with the magnetic field, the potential energy of a magnetic moment  $\mu$  in a magnetic field  $\mathbf{B}$ , is  $-\mu \cdot \mathbf{B}$ . Quantum mechanically,  $\mu = g\mu_B \mathbf{J} / \hbar$  where  $g$  is the Landé  $g$ -factor,  $\mu_B$  is the Bohr magneton and  $\mathbf{J}$  is the total angular momentum. This treatment will assume that orbital angular momentum  $\mathbf{L}$  is completely quenched by the crystal fields (i.e.  $\mathbf{L} = 0$ ), so the potential energy term, (also in units of  $\hbar$ ), is given by  $g\mu_B \mathbf{B} \cdot \sum_{i=1}^N \mathbf{S}_i$ . If we take the  $\mathbf{B}$  field as

defining the  $z$ -axis, then the magnetic field energy term is given by  $g\mu_B B \sum_{i=1}^N S_i^z$ , where  $S_i^z$  is the  $z$ -component of the spin at site  $i$ . For later convenience and without any loss of generality, we define  $m = -g\mu_B$  and thus the total Hamiltonian is given by

$$\mathcal{H} = -J \sum_{i=1}^N \mathbf{S}_i \cdot \mathbf{S}_{i+1} - mB \sum_{i=1}^N S_i^z. \quad (3.1)$$

Now the classical spin approximation, (which is necessarily invalid at low temperatures), recognizes that quantum spins of spin quantum number  $S$  can orient in  $2S + 1$  directions in real space. The spin vectors have length  $\sqrt{S(S+1)}$  in units of  $\hbar$ . We now

replace the quantum spins  $S_i \rightarrow \sqrt{S(S+1)}s_i$  by classical vectors of length  $\sqrt{S(S+1)}$ , where  $s_i$  is a unit vector at site  $i$ , free to point in any direction.

The classical Heisenberg Hamiltonian is now

$$\mathcal{H} = -JS(S+1)\sum_{i=1}^N \mathbf{s}_i \cdot \mathbf{s}_{i+1} - mB\sqrt{S(S+1)}\sum_{i=1}^N s_i^z. \quad (3.2)$$

To simplify the notation, establish effective dimensionless coupling constants and create simplified Boltzmann factors, we will define  $K \equiv \beta JS(S+1) \equiv JS(S+1)/(k_B T)$ , where  $T$  is the absolute temperature and  $k_B = 1.38 \times 10^{-23} \text{ J} \cdot \text{K}^{-1}$ . Similarly, we define  $L \equiv \beta mB\sqrt{S(S+1)} \equiv mB\sqrt{S(S+1)}/k_B T$ . The Boltzmann factor, from statistical mechanics is then expressed as,

$$\exp(-\beta\mathcal{H}) = \exp\left(K\sum_{i=1}^N \mathbf{s}_i \cdot \mathbf{s}_{i+1} + L\sum_{i=1}^N s_i^z\right). \quad (3.3)$$

The partition function as the sum of the Boltzmann factors becomes an integral since the classical spins are continuous,

$$Z = \int \dots \int \prod_{i=1}^N ds_i \exp(-\beta\mathcal{H}) = \int \dots \int \prod_{i=1}^N ds_i \exp\left(K\sum_{i=1}^N \mathbf{s}_i \cdot \mathbf{s}_{i+1} + L\sum_{i=1}^N s_i^z\right), \quad (3.4)$$

where  $ds_i = \sin\theta_i d\theta_i d\phi_i$ , is the element of solid angle about "spin"  $s_i$ . In parallel with our treatment of the Ising model in Chapter I, since the spins are classical variables, and hence commute with each other, we can express the exponential of the sum in (3.4) as a product of exponentials,

$$Z = \int \dots \int \prod_{i=1}^N ds_i T(s_1, s_2) T(s_2, s_3) \dots T(s_{N-1}, s_N) T(s_N, s_1), \quad (3.5)$$

where  $T(s, s')$  is the transfer operator. In what follows, we examine some of the mathematical properties of the transfer operator. We then show that knowledge of the eigenvalues of  $T$  enable us to find the partition function.

One way to write  $T(s, s')$  is as a symmetric function of its arguments,

$$T(s, s') = \exp\left(Ks \cdot s' + \frac{1}{2}L(s^2 + s'^2)\right). \quad (3.6)$$

This form is not necessary, however; one could also contrive the following non-symmetric transfer operators:

$$T_+(s, s') = \exp(Ks \cdot s' + Ls^2) \quad \text{or} \quad T_-(s, s') = \exp(Ks \cdot s' + Ls'^2); \quad (3.7)$$

these non-symmetric operators are in fact transpose pairs since  $T_+(s', s) = T_-(s, s')$ .

In Chapter III, Section E we will return to these non-symmetric forms of  $T$ . Here we will explore the mathematical consequences of employing the symmetric version of  $T$ , (3.6).

If we consider the integral equation

$$\int ds' T(s, s') \psi_n(s') = \lambda_n \psi_n(s), \quad (3.8)$$

this defines the eigenfunctions  $\psi_n(s)$  and eigenvalues  $\lambda_n$  of  $T$ , where  $n=1, 2, \dots$  is a discrete index. If  $T(s, s')$  is symmetric, (e.g. equation (3.6)), then Hilbert-Schmidt theory [Ref.29] guarantees that the eigenvectors are a complete orthonormal set and that the eigenvalues are real. The completeness and orthonormality of the eigenvectors on the unit sphere means:

$$\int ds \psi_n^*(s) \psi_m(s) = \delta_{nm} \quad (\text{orthonormal}) \quad \text{and} \quad (3.9a)$$

$$\sum_{n=1}^{\infty} \psi_n^*(s) \psi_n(s') = \delta(s - s') \quad (\text{complete}) \quad (3.9b)$$

It is shown in the theory of integral equations [Ref.29] that because (3.6) is real and

symmetric, we may expand the transfer operator in terms of its eigenvalues and eigenvectors,

$$T(s, s') = \sum_{n=1}^{\infty} \lambda_n \psi_n(s) \psi_n^*(s'). \quad (3.10)$$

With this expansion, one can show that the partition function for the N-spin system is given by,

$$Z_N = \sum_{n=1}^{\infty} \lambda_n^N. \quad (3.11)$$

To see how (3.11) arises, let us work out the details for the case of the N=2 system. Starting from (3.5) we have

$$Z_2 = \int \int_{s_1 s_2} ds_1 ds_2 T(s_1, s_2) T(s_2, s_1). \quad (3.12)$$

Substituting the expansion (3.10) in (3.12), we have

$$\begin{aligned} Z_2 &= \int \int_{s_1 s_2} ds_1 ds_2 \sum_{n=1}^{\infty} \lambda_n \psi_n(s_1) \psi_n^*(s_2) \sum_{m=1}^{\infty} \lambda_m \psi_m(s_2) \psi_m^*(s_1) \\ &= \sum_{n,m=1}^{\infty} \lambda_n \lambda_m \int_{s_1} ds_1 \psi_n(s_1) \psi_m^*(s_1) \int_{s_2} ds_2 \psi_n^*(s_2) \psi_m(s_2) = \sum_{n,m=1}^{\infty} \lambda_n \lambda_m \delta_{n,m} \\ Z_2 &= \sum_{n=1}^{\infty} \lambda_n^2, \end{aligned} \quad (3.13)$$

where we have used the orthonormality properties given in (3.9a). It is thus clear how to extend the treatment to general values of N and arrive at (3.11). Just as we obtained in the analysis of the Ising model, obtaining the partition function of the classical Heisenberg system is tantamount to finding the eigenvalues of the transfer operator.

### C. ZERO-FIELD EIGENVALUES

At this point, it will be useful to show how one may obtain analytically the eigenfunctions and eigenvalues of  $T$  for zero applied magnetic field. The key to the subsequent development is the use of the following expansion

$$\exp(K\mathbf{s}_1 \cdot \mathbf{s}_2) = 4\pi \sum_{l=0}^{\infty} \sum_{m=-l}^l f_l(K) Y_{l,m}(\mathbf{s}_1) Y_{l,m}^*(\mathbf{s}_2), \quad (3.14)$$

where 
$$f_l(K) = \sqrt{\frac{\pi}{2K}} I_{l+\frac{1}{2}}(K), \quad (3.15)$$

is a modified spherical Bessel function and  $Y_{l,m}$  is the standard spherical harmonic function. For future reference in characterizing matrix symmetry, we note the Bessel function parity property  $f_l(-K) = (-1)^l f_l(K)$ . In addition, another essential result, commonly called the Condon Shortley phase convention, is the fact that the spherical harmonics obey  $Y_{l,m}^* = (-1)^m Y_{l,-m}$ . In what follows, we will work with spherical polar coordinates  $(\theta, \phi)$ . The angle between the two "spins" (unit vectors) is given by

$$\mathbf{s}_1 \cdot \mathbf{s}_2 = \cos \Theta = \cos \theta_1 \cos \theta_2 + \sin \theta_1 \sin \theta_2 \cos(\phi_1 - \phi_2), \quad (3.16)$$

which is a standard result from vector analysis. We will use the shorthand notation  $Y_{l,m}(s)$  to denote  $Y_{l,m}(\theta, \phi)$ . Equation (3.14) follows from combining two results from mathematics. The first is the expansion,

$$\exp(z \cos \theta) = \sum_{l=0}^{\infty} (2l+1) f_l(z) P_l(\cos \theta), \quad (3.17)$$

which is a special case of the Gegenbauer addition theorem for Bessel functions.

The second is the addition theorem for spherical harmonics,

$$P_l(\cos \Theta) = \frac{4\pi}{2l+1} \sum_{m=-l}^l Y_{l,m}(\theta_1, \phi_1) Y_{l,m}^*(\theta_2, \phi_2). \quad (3.18)$$

Combining (3.17) and (3.18) leads to (3.14).

Comparing (3.14) with (3.10), we can identify the eigenvalues of T as

$$\lambda_{l,m} = 4\pi f_l(K). \quad \text{Note that in this zero-field case each eigenvalue is } (2l+1)\text{-fold}$$

degenerate. When we turn on a B field, the degeneracy is lifted. We also identify the eigenfunction of T in the zero-field limit as  $\psi_{l,m}(s) = Y_{l,m}(s)$ . Note that, as opposed to (3.8) in which a single generic index is used to label the eigenfunctions, in this case we must employ two indices to label the eigenfunctions and eigenvalues. We can verify that the  $Y_{l,m}$ 's are the correct eigenfunctions with the  $f_l(K)$ 's as the eigenvalues as follows.

Let's assume this assertion to be true and substitute into the eigenvalue integral equation,

$$\int \exp(Ks_1 \cdot s_2) Y_{l',m'}(s_2) ds_2 = \lambda_{l',m'} Y_{l',m'}(s_1). \quad (3.19)$$

Now employing the expansion (3.14), and the (3.9a) orthonormality property we have

$$\begin{aligned} 4\pi \int ds_2 \sum_{l,m} f_l(K) Y_{l,m}(s_1) Y_{l,m}^*(s_2) Y_{l',m'}(s_2) &= 4\pi \sum_{l,m} f_l(K) Y_{l,m}(s_1) \int ds_2 Y_{l,m}^*(s_2) Y_{l',m'}(s_2) \\ &= 4\pi \sum_{l,m} f_l(K) Y_{l,m}(s_1) \delta_{l,l'} \delta_{m,m'} = 4\pi f_{l',m'}(K) Y_{l',m'}(s_1). \end{aligned} \quad (3.20)$$

Thus, as demonstrated by Joyce [Ref. 7], in zero applied field, the partition function is

$$Z_N(K) = (4\pi)^N \sum_{l=0}^{\infty} (2l+1) f_l^N(K). \quad (3.21)$$

We can check that (3.21) properly reduces to the correct high-temperature limit

$$Z_N(0) = (4\pi)^N \quad \text{upon using the property of the modified spherical Bessel function}$$

$$f_l(0) = \delta_{l,0}.$$

#### D. BLUME, HELLER, AND LURIE METHODOLOGY

Published in 1975 [Ref. 8], this numerical method achieved the first theoretical results of the thermodynamic properties for the classical Heisenberg magnetic chain in an applied magnetic field. Using the transfer matrix method and numerical Gaussian integration, this achievement extended the zero field analytic solution of Joyce to the non-zero field case. In a magnetic field, formulating a numerical evaluation of the eigenfunction, Blume *et al* [Ref. 8] first noted that the eigenfunction can, by symmetry, be written in the form  $\Psi_{l,m}(s) = \psi_{l,m}(\cos\theta) \left( \frac{1}{\sqrt{2\pi}} \right) e^{im\phi}$ , where  $\theta$  and  $\phi$  are the polar and azimuthal angles respectively of spin  $s$ . This separation of variables recognizes that even in the presence of an external field, the azimuthal parameter  $m$  remains a good quantum number. Letting  $x = \cos\theta$ , utilizing (3.16), and using the symmetric kernel (3.6), equation (3.8) (with indices  $l,m$  in lieu of  $n$ ) becomes,

$$\int_{-1}^1 dx' \int_0^{2\pi} d\phi' \exp \left( Kx x' + K \left[ (1-x^2)(1-x'^2) \right]^{\frac{1}{2}} \cos(\phi - \phi') + \frac{L}{2}(x+x') \right) \times \psi_{l,m}(x') \frac{e^{im\phi'}}{\sqrt{2\pi}} = \lambda_{l,m} \psi_{l,m}(x) \frac{1}{\sqrt{2\pi}} e^{im\phi}. \quad (3.22)$$

The integral over  $\phi'$  can be carried out analytically with the result,

$$2\pi \int_{-1}^1 dx' \exp \left( Kx x' + \frac{L}{2}(x+x') \right) I_m \left( K \left[ (1-x^2)(1-x'^2) \right]^{\frac{1}{2}} \right) \psi_{l,m}(x') dx' = \lambda_{l,m} \psi_{l,m}(x). \quad (3.23)$$

Here  $I_m(x) = \frac{1}{2\pi} \int_0^{2\pi} \exp(x \cos\phi - im\phi) d\phi = I_m(-x) = I_{-m}(x)$  is the Bessel function of

imaginary argument. This one-dimensional integral equation can now be solved numerically by converting it to a matrix equation. The integral over  $x'$  is performed by

$N_I$ -point Gaussian integration, using the approximation  $\int_{-1}^{+1} f(x) dx \approx \sum_{j=1}^{N_I} w_j f(x_j)$ , where

the weights  $w_j$  and the points  $x_j$  are tabulated.[Ref. 30] The integral equation then

becomes,

$$\int_{-1}^{+1} dx' G_m(x, x') \psi_{lm}(x') = \lambda_{lm} \psi_{lm}(x) \approx \sum_{j=1}^{N_I} w_j G_m(x, x_j) \psi_{lm}(x_j), \quad (3.24)$$

where  $G_m(x, x') = 2\pi e^{Kxx' + \frac{L}{2}(x+x')}$   $I_m\left(K\left[(1-x^2)(1-x'^2)\right]^{1/2}\right)$ . If we look for solutions of Eq.

(3.23) only at the points  $x = x_i$  of the numerical integration, the integral equation

becomes a matrix eigenvalue equation:  $\sum_j w_j G_m(x_i, x_j) \psi_{lm}(x_j) = \lambda_{lm} \psi_{lm}(x_i)$ . To make

this more symmetric, we multiply both sides of the equation by  $\sqrt{w_i}$ , obtaining

$$\sum_{j=1}^{N_I} \mathcal{A}_{ij}^{(m)} \phi_j^{(lm)} = \lambda_{lm} \phi_i^{lm}, \quad (3.25)$$

where  $\mathcal{A}_{ij}^{(m)} = \sqrt{w_i} G_m(x_i, x_j) \sqrt{w_j}$  and  $\phi_i^{(lm)} = \sqrt{w_i} \psi_{lm}(x_i)$ . Equation (3.25) is an

$N_I \times N_I$  matrix eigenvalue equation with  $N_I$  determined by the number of points used in

the numerical integration. As stated in the introduction, (and assuredly worth repeating),

a value of  $N_I=16$  suffices to give convergence to seven significant figures for all values

of  $K$  and  $L$ . The largest eigenvalue of equation (3.25) occurs for  $m=0$ . This is in

consonance with the fact that the eigenfunction belonging to the largest eigenvalues has

no nodes. In a sufficiently large spin system, only the largest eigenvalue survives, that is

$Z \rightarrow \lambda_0^N$  for  $N \rightarrow \infty$ . The free energy appropriate to an infinite-site system can be

obtained from this eigenvalue and other thermodynamic quantities can be found by

numerical differentiation with respect to the appropriate variables.

## E. REPRESENTATION IN SPHERICAL HARMONICS

Mark Auslender, an Israeli physicist, has suggested, in a private communication, [Ref. 9], an alternate numerical strategy for solving the eigenvalue problem associated with the transfer-operator, (3.8). Auslender's suggestion consists of representing the transfer operator in terms of a spherical harmonic basis set. Since the spherical harmonics are the eigenvectors of the transfer operator for *zero* magnetic field, it is possible that Auslender's suggestion could prove numerically more efficient or flexible than the Gaussian integration approach discussed above for the case of non-zero magnetic field. We stress that Auslender has merely suggested this approach; we are here working out the details.

Thus, we first expand the eigenfunctions of  $T$  in terms of spherical harmonics,

$$\psi_n(s) = \sum_{l',m'} C_{l',m'}^{(n)} Y_{l',m'}(s). \quad (3.26)$$

Substituting (3.26) into (3.8), we have

$$\sum_{l',m'} C_{l',m'}^{(n)} \int ds' T(s, s') Y_{l',m'}(s') = \lambda_n \sum_{l',m'} C_{l',m'}^{(n)} Y_{l',m'}(s) \quad (3.27)$$

Then, multiplying (3.27) by  $Y_{l,m}^*(s)$  and integrating over  $s$ , we obtain

$$\sum_{l',m'} C_{l',m'}^{(n)} \int ds \int ds' Y_{l,m}^*(s) T(s, s') Y_{l',m'}(s') = \lambda_n C_{l,m}^{(n)}. \quad (3.28)$$

We now define the matrix elements,

$$T(l, m; l', m') = \iint ds ds' Y_{l,m}^*(s) T(s, s') Y_{l',m'}(s'), \quad (3.29)$$

in terms of which (3.28) becomes

$$\sum_{l',m'} T(l, m; l', m') C_{l',m'}^{(n)} = \lambda_n C_{l,m}^{(n)}. \quad (3.30)$$

For each  $n=1,2,\dots$ , (3.30) has the form of a matrix eigenvalue problem. In what follows, we will simplify our notation and suppress the index  $n$ . As previously, the goal will be to obtain the eigenvalues of  $T$ , now in a matrix representation given by (3.29).

The form of (3.30), however, is slightly unusual because the components of the eigenvectors are labeled by a double index set. We can cast (3.30) into standard form by lining up all of the eigenvector components into a column vector,

$$\mathbf{C} = \begin{pmatrix} C_{0,0} \\ C_{1,1} \\ C_{1,0} \\ C_{1,-1} \\ C_{2,2} \\ \vdots \end{pmatrix} \quad (3.31)$$

The column vector  $\mathbf{C}$  is infinite dimensional and the eigenvalue condition becomes a matrix eigenvalue equation,  $\mathbf{T} \cdot \mathbf{C} = \lambda \mathbf{C}$ , where  $\mathbf{T}$  is an infinite-dimensional matrix, the first few elements of which would be,

$$\mathbf{T} = \begin{pmatrix} T(0,0;0,0) & T(0,0;1,1) & T(0,0;1,0) & T(0,0;1,-1) & T(0,0;2,2) & \dots \\ T(1,1;0,0) & T(1,1;1,1) & T(1,1;1,0) & T(1,1;1,-1) & T(1,1;2,2) & \dots \\ T(1,0;0,0) & T(1,0;1,1) & T(1,0;1,0) & T(1,0;1,-1) & T(1,0;2,2) & \dots \\ T(1,-1;0,0) & T(1,-1;1,1) & T(1,-1;1,0) & T(1,-1;1,-1) & T(1,-1;2,2) & \dots \\ T(2,2;0,0) & T(2,2;1,1) & T(2,2;1,0) & T(2,2;1,-1) & T(2,2;2,2) & \dots \\ \vdots & \vdots & \vdots & \vdots & \vdots & \ddots \end{pmatrix} \quad (3.32)$$

We have thus formally reduced the integral eigenvalue equation (3.8) to a matrix eigenvalue equation, where, however, the matrix is infinite dimensional. Clearly, some practical means of truncating the matrix must be developed. This remains to be done.

We note that, in principle, the Gaussian integration scheme also produces an infinite

matrix to diagonalize. There it was found empirically, that a 16 x 16 matrix produced satisfactory results.

It will be instructive to first evaluate the matrix elements of  $T$  for the case of zero magnetic field by substituting (3.14) in (3.29)

$$\begin{aligned}
T(l, m; l', m') &= \int ds \int ds' Y_{l, m}^*(s) T(s, s') Y_{l', m'}(s') \\
&= \int ds \int ds' Y_{l, m}^*(s) \exp(Ks \cdot s') Y_{l', m'}(s') \\
&= 4\pi \sum_{l_1, m_1} f_{l_1}(K) \int ds \int ds' Y_{l, m}^*(s) Y_{l_1, m_1}(s) Y_{l_1, m_1}^*(s') Y_{l', m'}(s') \\
&= 4\pi \sum_{l_1, m_1} f_{l_1}(K) \delta_{l_1, l} \delta_{m_1, m} \delta_{l_1, l'} \delta_{m_1, m'} \\
&= 4\pi f_l(K) \delta_{l, l'} \delta_{m, m'}.
\end{aligned} \tag{3.33}$$

Not surprisingly, yet reassuringly, this shows the matrix is diagonal with the zero field eigenvalues along the diagonal.

To incorporate the magnetic field into the matrix construction, either a symmetric or a non-symmetric approach is possible. We will explore both avenues, but before proceeding, we list the following results that will prove useful in our subsequent analysis.

The first derives from the addition theorem for Legendre polynomials:

$$\exp(Ls^2) = \exp(L \cos \theta) = \sqrt{4\pi} \sum_{j=0}^{\infty} \sqrt{2j+1} f_j(L) Y_{j,0}(s). \quad [\text{Ref. 30 p.445}] \tag{3.34}$$

We will also require the general integral over three spherical harmonics,

$$\int ds Y_{l_1, m_1}(s) Y_{l_2, m_2}(s) Y_{l_3, m_3}(s) = \sqrt{\frac{(2l_1+1)(2l_2+1)(2l_3+1)}{4\pi}} \begin{pmatrix} l_1 & l_2 & l_3 \\ 0 & 0 & 0 \end{pmatrix} \begin{pmatrix} l_1 & l_2 & l_3 \\ m_1 & m_2 & m_3 \end{pmatrix} \tag{3.35}$$

where  $\begin{pmatrix} l_1 & l_2 & l_3 \\ m_1 & m_2 & m_3 \end{pmatrix}$  is the Wigner 3j-symbol. [Ref. 31 p63] The Wigner 3j symbol

is a symmetric form of the Clebsch-Gordan coefficient that arises frequently in contexts

involving coupling of angular momenta in quantum mechanics and other applications of the rotation group. The  $3j$  symbols are non-zero only when  $m_1 + m_2 + m_3 = 0$  and the top row satisfies a triangle condition,  $|l_1 - l_2| \leq l_3 \leq l_1 + l_2$ . When the bottom row is identically zero, there is an additional rule that the top row must sum to an even integer.

### 1. The Symmetric Kernel

Since (3.6), the original transfer operator  $T(s, s')$  is symmetric, we expect the matrix  $\mathbf{T}$  to be Hermitian. This will ensure that the eigenvalues  $\lambda$  are real. Following (3.29), we need to evaluate the matrix elements,

$$\begin{aligned} T(l, m; l', m') &= \int ds \int ds' Y_{l,m}^*(s) T(s, s') Y_{l',m'}(s') \\ &= \int ds \int ds' Y_{l,m}^*(s) \exp(Ks \cdot s' + \frac{1}{2}L(s^2 + s'^2)) Y_{l',m'}(s'). \end{aligned} \quad (3.36)$$

We now substitute in the expansions (3.14) and (3.34),

$$\exp(Ks \cdot s') = 4\pi \sum_{l,m} f_l(K) Y_{l,m}(s) Y_{l,m}^*(s') \quad \text{and} \quad (3.14)$$

$$\exp\left(\frac{1}{2}Ls^2\right) = \sqrt{4\pi} \sum_{l=0}^{\infty} f_l(L/2) \sqrt{2l+1} Y_{l,0}(s). \quad (3.34)$$

The expression for the matrix element then becomes,

$$\begin{aligned} T(l, m; l', m') &= \int ds \int ds' Y_{l,m}^*(s) \exp(Ks \cdot s' + \frac{1}{2}L(s^2 + s'^2)) Y_{l',m'}(s') \\ &= \int ds \int ds' Y_{l,m}^*(s) \left[ 4\pi \sum_{l_1, m_1} f_{l_1}(K) Y_{l_1, m_1}^*(s') Y_{l_1, m_1}(s) \right] \\ &\times \left[ \sqrt{4\pi} \sum_{l_2=0} f_{l_2}(L/2) \sqrt{2l_2+1} Y_{l_2,0}(s) \right] \left[ \sqrt{4\pi} \sum_{l_3=0} f_{l_3}(L/2) \sqrt{2l_3+1} Y_{l_3,0}(s') \right] Y_{l',m'}(s'). \end{aligned}$$

Collecting terms, we have,

$$T(l, m; l', m') = (4\pi)^2 \sum_{l_1, m_1} \sum_{l_2} \sum_{l_3} f_{l_1}(K) f_{l_2}(L/2) \sqrt{2l_2+1} f_{l_3}(L/2) \sqrt{(2l_3+1)} \\ \times \left( \int ds Y_{l,m}^*(s) Y_{l_1, m_1}(s) Y_{l_2, 0}(s) \right) \left( \int ds' Y_{l_1, m_1}^*(s') Y_{l_3, 0}(s') Y_{l', m'}(s') \right). \quad (3.37)$$

Employing (3.25), the integral over 3 spherical harmonics and using the fact that

$Y_{l,m}^* = (-1)^m Y_{l,-m}$ , we obtain the ponderous expression,

$$T(l, m; l', m') = (4\pi)^2 \sum_{l_1, m_1} \sum_{l_2} \sum_{l_3} f_{l_1}(K) f_{l_2}(L/2) \sqrt{2l_2+1} f_{l_3}(L/2) \sqrt{(2l_3+1)} (-1)^m (-1)^{m_1} \\ \times \left( \frac{(2l+1)(2l_1+1)(2l_2+1)}{4\pi} \right)^{1/2} \begin{pmatrix} l & l_1 & l_2 \\ 0 & 0 & 0 \end{pmatrix} \begin{pmatrix} l & l_1 & l_2 \\ -m & m_1 & 0 \end{pmatrix} \\ \times \left( \frac{(2l_1+1)(2l_3+1)(2l'+1)}{4\pi} \right)^{1/2} \begin{pmatrix} l_1 & l_3 & l' \\ 0 & 0 & 0 \end{pmatrix} \begin{pmatrix} l_1 & l_3 & l' \\ -m_1 & 0 & m' \end{pmatrix}.$$

We can simplify this beast somewhat,

$$T(l, m; l', m') = (4\pi) \sum_{l_1, m_1} \sum_{l_2} \sum_{l_3} f_{l_1}(K) f_{l_2}(L/2) f_{l_3}(L/2) (2l_1+1)(2l_2+1)(2l_3+1) \sqrt{(2l+1)(2l'+1)} \\ \times \begin{pmatrix} l & l_1 & l_2 \\ 0 & 0 & 0 \end{pmatrix} \begin{pmatrix} l & l_1 & l_2 \\ -m & m_1 & 0 \end{pmatrix} \begin{pmatrix} l_1 & l_3 & l' \\ 0 & 0 & 0 \end{pmatrix} \begin{pmatrix} l_1 & l_3 & l' \\ -m_1 & 0 & m' \end{pmatrix} (-1)^{m+m_1}. \quad (3.38)$$

Utilizing the properties of the  $3j$  symbol discussed above, we have for the symbols

appearing in (3.38),

$$\begin{pmatrix} l & l_1 & l_2 \\ -m & m_1 & 0 \end{pmatrix} = \delta_{m, m_1} \begin{pmatrix} l & l_1 & l_2 \\ -m & m & 0 \end{pmatrix} \\ \begin{pmatrix} l_1 & l_3 & l' \\ -m_1 & 0 & m' \end{pmatrix} = \delta_{m', m_1} \begin{pmatrix} l_1 & l_3 & l' \\ -m' & 0 & m' \end{pmatrix}$$

We can thus instantly sum over  $m_1$ , (using the fact that  $\sum_{m_1} \delta_{m_1, m} \delta_{m_1, m'} = \delta_{m, m'}$ ), and the

matrix elements become,

$$T(l, m, l', m') = 4\pi\delta_{m, m'} \sqrt{(2l+1)(2l'+1)} \sum_{l_1}^{\infty} \sum_{l_2=0}^{\infty} \sum_{l_3=0}^{\infty} f_{l_1}(K) f_{l_2}(L/2) f_{l_3}(L/2) (2l_1+1)(2l_2+1)(2l_3+1) \\ \times \begin{pmatrix} l & l_1 & l_2 \\ 0 & 0 & 0 \end{pmatrix} \begin{pmatrix} l & l_1 & l_2 \\ -m & m & 0 \end{pmatrix} \begin{pmatrix} l_1 & l_3 & l' \\ 0 & 0 & 0 \end{pmatrix} \begin{pmatrix} l_1 & l_3 & l' \\ -m & 0 & m \end{pmatrix} \quad (3.39)$$

Equation (3.39) seemingly involves a triple infinite sum. The "triangle" properties of the  $3j$  symbols probably restrict some or all of these summations to be finite sums. We will not further analyze (3.39) because, as it turns out, a considerably simpler expression for the matrix elements can be obtained by working with the asymmetric form of the transfer operator (3.7) mentioned in chapter III, section A.

## 2. The Non-Symmetric Kernel

We now obtain the matrix elements associated with the asymmetric form of the transfer operator,  $T(s, s') = \exp(Ks \cdot s' + Ls^2)$ . First, however, we note that one might be concerned that a non-symmetric kernel would not have real eigenvalues. (Recall, as discussed above, that Hilbert-Schmidt theory guarantees that a real symmetric kernel has real eigenvalues). In this particular case, however, we can show that the non-symmetric kernel is related to the symmetric form of the kernel by a similarity transformation, and hence has the same eigenvalues as the symmetric kernel. Consider that the eigenvalue equation, (3.8), is equivalent to the following

$$\int g(s) T(s, s') g^{-1}(s') g(s') \psi_n(s') ds' = \lambda_n g(s) \psi_n(s) \quad (3.8')$$

$$\text{or} \quad \int \tilde{T}(s, s') \tilde{\psi}_n(s') ds' = \lambda_n \tilde{\psi}_n(s)$$

$$\text{where } \tilde{T}(s, s') \equiv g(s) T(s, s') g^{-1}(s') \quad \text{and} \quad \tilde{\psi}_n(s) \equiv g(s) \psi_n(s).$$

So long as a function  $g(s)$  can be found such that  $\tilde{T}$  is symmetric,  $T$  and  $\tilde{T}$  will have the same (real) eigenvalues. In our case, it is easy to find the transformation function,  $g(s) = \exp(-Ls/2)$ . Thus, the (3.7) non-symmetric kernels  $T_{\pm}(s, s')$  have the same eigenvalues as the (3.6) symmetric  $T(s, s')$ .

Utilizing now  $T_+(s, s')$  from (3.7), we have from (3.29),

$$\begin{aligned}
T(l, m; l', m') &= \iint ds ds' Y_{l, m}^*(s) \exp(Ks \cdot s' + Ls^2) Y_{l', m'}(s') \\
&= (4\pi)^{3/2} \sum_{l_1, m_1} \sum_{j=0}^{\infty} f_{l_1}(K) f_j(L) \sqrt{2j+1} \left( \int ds Y_{l_1, m_1}^*(s) Y_{l_1, m_1}(s) Y_{j, 0}(s) \right) \\
&\quad \times \left( \int ds' Y_{l_1, m_1}^*(s') Y_{l', m'}(s') \right) \\
&= (4\pi)^{3/2} f_r(K) \sum_{j=0}^{\infty} f_j(L) \sqrt{2j+1} \left( \int ds Y_{l, m}^*(s) Y_{l', m'}(s) Y_{j, 0}(s) \right) \\
&= 4\pi f_r(K) \sqrt{(2l+1)(2l'+1)} (-1)^m \sum_{j=0}^{\infty} f_j(L) (2j+1) \begin{pmatrix} l & l' & j \\ 0 & 0 & 0 \end{pmatrix} \begin{pmatrix} l & l' & j \\ -m & m' & 0 \end{pmatrix}
\end{aligned} \tag{3.40}$$

where, in arriving at the last line, we have used the phase convention that

$Y_{l, m}^* = (-1)^m Y_{l, -m}$ . We now utilize the "selection rule" properties of the  $3j$ -symbols: The  $3j$ -symbols are non-zero only when the sum of the bottom row is zero, and when the upper row satisfies the triangle inequality,  $|l - l'| \leq j \leq l + l'$ . These two facts: (1) restrict the sum over  $j$ , and, (2), makes the matrix element diagonal in the variable  $m$ :

$$T(l, m; l', m') = 4\pi (-1)^m \delta_{m, m'} f_r(K) \sqrt{(2l+1)(2l'+1)} \sum_{j=|l-l'|}^{l+l'} f_j(L) (2j+1) \begin{pmatrix} l & l' & j \\ 0 & 0 & 0 \end{pmatrix} \begin{pmatrix} l & l' & j \\ -m & m & 0 \end{pmatrix} \tag{3.41}$$

We note the additional rule for  $3j$ -symbols that when the bottom row is all zero, the symbol is non-zero only when the upper row sums to an even integer. Thus, the sum over  $j$  in (3.41) is further restricted to values such that  $l + l' + j = 2p$ , where  $p$  is an integer. We note that the fact that  $T(l, m; l', m')$  is diagonal in  $m$ , makes sense; the

azimuthal quantum number remains a good quantum number in the presence of the field.

Finally, we note that utilizing the other asymmetric form for the kernel

$$(T(s, s') = \exp(Ks \cdot s' + Ls'^z)) \text{ merely produces the transpose of } T(l, m; l', m').$$

It is easy to verify that the correct zero-field limit results from (3.41). Using the fact that  $f_j(0) = \delta_{j,0}$  and the  $3j$ -symbol,

$$\begin{pmatrix} l & l & 0 \\ -m & m & 0 \end{pmatrix} = \frac{(-1)^{l-m}}{\sqrt{2l+1}},$$

we obtain the zero-field limit,  $T(l, m; l', m') = 4\pi f_l(K) \delta_{l,l'} \delta_{m,m'}$  as derived previously (3.33).

One can also show that (3.39) properly reduces to (3.33) in the zero-field limit.

Using the symmetry properties of the  $3j$ -symbols, it is simple to show that the transpose of  $T(l, m; l', m')$  is given by,  $T(l', m'; l, m) = [f_l(K)/f_{l'}(K)] T(l, m; l', m')$ .

Since we started from an asymmetric version of the transfer operator, it is not surprising that  $\mathbf{T}$  is not symmetric. We note that the transpose relation implies that the matrix elements have the symmetry property,  $f_{l'} T(l', m'; l, m) = f_l T(l, m; l', m')$ .



## IV. DISCUSSION

The purpose of this thesis has been to investigate a method for obtaining the thermodynamic partition function for classical Heisenberg spins that interact with isotropic nearest-neighbor exchange interactions and which are coupled to an external magnetic field. Equation (3.41) is the main result of this thesis. It provides an expression for the matrix elements of the transfer operator for classical Heisenberg spins that result upon utilizing a basis of spherical harmonic functions. The motivation for pursuing this new matrix representation is ultimately to assess its numerical efficiency, as compared with Blume's Gaussian quadrature method, in determining the eigenvalues of the transfer operator. Within the transfer matrix formalism for calculating the equilibrium properties of interacting spins on a lattice, the "matrix" in this case being an operator, the partition function is obtained from the eigenvalues of the transfer operator. We emphasize that the Gaussian integration method is the only other numerical method available in the physics literature of which we are aware for obtaining the eigenvalues of the transfer operator for classical Heisenberg spins in an external magnetic field. Moreover, we note that the transfer matrix method is the only general method for treating the statistical mechanics of interacting spins; there are only a handful of exceptional cases where the partition function can be obtained directly, without recourse to the transfer-matrix method.

As discussed in the introduction, great progress is being made in the ability to fabricate molecular clusters containing a small number of magnetic ions (e.g., as few as four). Recent advances in the fabrication of molecular magnets portend an unprecedented ability to control the placement of magnetic moments in molecular structures and hence to design and produce nanometer-scale magnetic systems. As

molecular magnetic systems continue to be explored for their possible applications, robust and reliable numerical methods will be required to model their thermodynamic properties. In the past, physicists have explored spin models for their ability to characterize phase transitions. Phase transitions and critical phenomena, however, require that the “thermodynamic limit” be taken at the end of the calculation, which, for spins on a lattice, means that the number of spins in the system becomes infinite, (i.e.,  $N \rightarrow \infty$ ). In this limit, only the largest eigenvalue of the transfer matrix becomes relevant. We note that specialized numerical methods exist for seeking either the smallest or the largest eigenvalue of a given matrix. For the development of nanomagnetism, however, we are concerned with the opposite limit to that attendant to the study of phase transitions, (i.e., here  $N \rightarrow \text{finite few}$ ). To obtain the partition function for systems with just a few magnetic atoms, we will require an indefinite number of the transfer matrix eigenvalues and hence it is worthwhile to explore new methods for calculating these quantities. We note that the number of eigenvalues of the transfer operator is independent of the size of the system. In some sense, we have entered an era of “applied statistical physics,” and appropriate tools are required.

Without a detailed numerical investigation, it is difficult to assess the utility of (3.41) *vis-à-vis* Gaussian quadrature. We can offer the following observations. First, it is exact. Equation (3.41) provides the *exact* matrix elements of the transfer operator in the basis of spherical harmonics, and this fact alone may offer insights. Stated differently, the Gaussian integration method is purely numerical, whereas (3.41) is based on an exact theoretical expression, which in and of itself may prove useful. Second, one hopes that (3.41) will prove advantageous at least for the case of relatively small magnetic fields.

Because (3.41) is diagonal for zero magnetic field, (since the spherical harmonics are the zero-field eigenfunctions of the transfer operator), one would expect for non-zero magnetic field that the off-diagonal terms would remain relatively small, and, moreover, to become progressively smaller as one proceeds away from the diagonal. This follows from the properties of the modified spherical Bessel functions in (3.41). These functions have the property that they become monotonically smaller as a function of the order for fixed values of the argument. In particular, when the value of the order exceeds the value of the argument, the value of the function vanishes (approximately) exponentially as an increasing function of the order. From (3.41), we see that the lower limit of the summation is given by  $|l - l'|$ , i.e., the order of the first (and largest) term in the summation is directly given by the distance to diagonal. Hopefully, such considerations will prove useful in developing "rules of thumb" for deciding how to truncate the matrix for the purpose of numerically obtaining the eigenvalues. In a similar way, we note that the number of terms to include *along* the diagonal is governed by the overall, field-independent, modified spherical Bessel function in (3.41) which is a function of  $K$ , the dimensionless nearest-neighbor coupling constant. It thus seems likely that with suitable numerical experimentation, one can develop practical schemes for truncating the matrix for given values of  $K$  and  $L$ . Finally, a decided advantage of (3.41) is that it provides a systematic way for increasing the accuracy of the eigenvalues, if such is desired. It was noted in Chapter III that a 16x16 matrix was sufficient to guarantee seven digit accuracy with Gaussian integration. It is a feature of Gaussian integration, however, that one cannot systematically obtain more accuracy by increasing the number of integration points. For numerical reasons, the accuracy of Gaussian integration "saturates" for a

relatively small number of integration points. Thus, while seven-digit accuracy is commendable, if for some reason one wanted higher accuracy, it could probably not be obtained using Gaussian integration.

As surmised at the outset, only performing the actual calculations will convey “the rest of the story”. In general, computational efficiency yardsticks, like the *means* of matrix truncation and the *ends* of convergence results, must of course await actual programming and calculation. Application accuracy, as well as flexibility are key factors in adjudging the utility of any tool. So it is with models; in this case the efficacy, versatility, and robustness of the spherical harmonic representation is yet to be determined. Although pragmatic results will remain the preeminent objective, when an intrinsically exact and high fidelity model formulation can engender an illustrative understanding of the phenomenon examined, this is a welcome bonus. Finally, as for the macromolecular magnetic frontier, the nanometer investigation and fabrication technologies undoubtedly will encourage a convergence of scientific disciplines. The chemist, physicist, and “nanotechnologist” will merge here to both gain an understanding and inevitably utilize these ultra-small complexes.

## LIST OF REFERENCES

1. Von Hippel, A.R. and collaborators, *Molecular Science and Molecular Engineering*, M.I.T. Press and Wiley & Sons, 1959
2. Chaiken, P.M. & Lubensky, T.C., *Principles of Condensed Matter Physics*, Cambridge University Press, pp. 464-477, 1995
3. Weiss, P., *J. Phys et Radium*, vol. 6, no. 667, 1907; *Physik.Z.* vol. 9, no. 358, 1908
4. Stanley, H.E., *Introduction to Phase Transitions and Critical Phenomena*, Chapter 8, Oxford University Press, 1971
5. Onsager, L., *Phys Rev.*, vol. 65, no. 117, 1944
6. Fisher, M.E., "The Heisenberg Model for Infinite Spin", *J. Math. Phys.*, vol. 5, no. 944, 1964
7. Joyce, G.S., "Classical Heisenberg Model", *Phys Rev.*, vol. 155, no. 2, 1967
8. Blume, M., "Classical One-Dimensional Heisenberg Magnet in an Applied Field", *Phys Rev B.*, vol. 11, no. 11, 1975
9. Auslender, M., A four page fax, dated 10 September, 1997, from author to Marshall Luban, a colleague of Jim Luscombe. The mathematical proposal is entitled "Heisenberg Chain-Transfer Matrix Method"
10. Pathria, R.K., *Statistical Mechanics*, Pergamon Press, 1972
11. Maris, H.J., and Kadanoff, L.P., "Teaching the Renormalization Group", *Am J Physics*, vol. 46, no. 6, June 1978
12. Chudnovsky, E.M., "Quantum Hysteresis in Molecular Magnets", *Science*, vol. 274, no. 8, November, 1996
13. Friedman, J.R. *et al*, "Macroscopic Measurement of Resonant Magnetization" Tunneling in High Spin Molecules", *Phys Rev Ltrs.*, vol. 76, no. 20, 13 May, 1996
14. Awschalom, D. and Vincenzo, D., "Complex Dynamics of Mesoscopic Magnets", *Physics Today*, April, 1995
15. Gatteschi, D. *et al*, "Large Clusters of Metal Ions: The Transition from Molecular to Bulk Magnets", *Science* vol. 265, pp. 1054-1058, August, 1994

16. Sessoli, R. *et al*, "Magnetic Bistability in a Metal Ion Cluster", *Nature*, vol. 365, September, 1993
17. Lascialfari, A., and Gatteschi, D. *et al*, "Spin Dynamics in Mesoscopic Size Magnetic Systems...", *Phys. Rev. B*, vol. 55, no. 21, 01 June, 1997
18. Tejada, J. *et al*, "Quantum Tunneling of Magnetization in Nano-structured Materials", *Chem Matter* vol. 8, pp. 1784-92, 1996
19. Zhang, X.X., *et al*, "Magnetic Relaxation and Quantum Tunneling in Nanocrystalline Particles", *J of Magnetism & Matter*, pp.140-144, 1995
20. Delfs, C.D. *et al*, *Inorganic Chemistry*, vol. 32, no. 3099, 1993
21. Luscombe, J.H. *et al*, "Classical Heisenberg Model of Magnetic Molecular Ring Clusters: Accurate Approximants for Correlation Functions and Susceptibility", *J of Chem Phys*, vol.108, no. 17, 1 May, 1998
22. Lascialfari, A. *et al*, "Proton NMR and  $\mu$ SR in  $Mn_{12}O_{12}$  Acetate: A Mesoscopic Magnetic Molecular Cluster", *Phys Rev B*, vol. 57, no. 1, 1 January, 1998
23. Kramer, H. and Wannier, G., "Statistics of a Two-Dimensional Ferromagnet", *Phys Rev*, vol. 60, Nos. 252,263. 1941
24. Von Hippel, A., *Dielectrics and Waves*, originally published, Wiley & Son, 1954, new edition, Artech House, 1995
25. Kittel, C., *Introduction to Solid State Physics*, second edition, John Wiley & Sons, Inc., 1956
26. Ashcroft, N. and Mermin, N., *Solid State Physics*, Holt, Rinehart, and Winston, 1976
27. "Illustration", *Britannica Online*. <<http://www.eb.com:180/cgi-in/g?DocF=micro/367/35.html>>
28. Bohm, D., *Quantum Theory*, Prentice-Hall, 1951, Dover ed. 1989, p. 489
29. Tricomi, F.G., *Integral Equations*, p. 110, Dover edition, 1985
30. Abramowitz, M., and Stegun, I.A., (ed), *Handbook of Mathematical Functions*, NBS, p. 916, Washington, 1964
31. Edmonds, A.R., *Angular Momentum in Quantum Mechanics*, Princeton University Press, 1974

## INITIAL DISTRIBUTION LIST

1. Defense Technical Information Center .....2  
8725 John J. Kingman Rd., STE 0944  
Ft. Belvoir, Virginia 2060-6218
2. Dudley Knox Library .....2  
Naval Postgraduate School  
4111 Dyer Rd.  
Monterey, California 93943-5101
3. James H. Luscombe, Code PH/LJ.....2  
Physics Department/Combat Systems Curriculum  
Naval Postgraduate School  
833 Dyer Rd.  
Monterey, California 93943-5101
4. Robert L. Armstead, Code PH/AR.....1  
Physics Department/Combat Systems Curriculum  
833 Dyer Rd.  
Monterey, California 93943-5101
5. John Montgomery.....2  
Naval Research Laboratory  
Mail Stop Code 5700.00  
Washington, D.C. 20375-5320
6. CDR Randall J. Franciose.....3  
6812 Sydenstricker Road  
Springfield, Virginia 22152